Title

Retinoic acid controls the homeostasis of pre-cDC–derived splenic and intestinal dendritic cells

Journal

Journal of Experimental Medicine, 210(10)

ISSN

0022-1007

Authors

Klebanoff, Christopher A
Spencer, Sean P
Torabi-Parizi, Parizad
et al.

Publication Date

2013-09-23

DOI

10.1084/jem.20122508

Peer reviewed

Retinoic acid controls the homeostasis of pre-cDC–derived splenic and intestinal dendritic cells

Christopher A. Klebanoff,[1,3] Sean P. Spencer,[4,6] Parizad Torabi-Parizi,[5,8] John R. Grainger,[4] Rahul Roychoudhuri,[3] Yun Ji,[2,3] Madhusudhanan Sukumar,[3] Pawel Muranski,[3] Christopher D. Scott,[3] Jason A. Hall,[4,6] Gabriela A. Ferreyra,[7,8] Anthony J. Leonardi,[3] Zachary A. Borman,[3] Jinshan Wang,[9] Douglas C. Palmer,[3] Christoph Wilhelm,[4] Rongman Cai,[7,8] Junfeng Sun,[7,8] Joseph L. Napoli,[9] Robert L. Danner,[7,8] Luca Gattinoni,[2,3] Yasmine Belkaid,[4] and Nicholas P. Restifo[3]

[1]Clinical Investigator Development Program and [2]Experimental Transplantation and Immunology Branch, [3]Center for Cancer Research, National Cancer Institute, National Institutes of Health (NIH), Bethesda, MD 20892
[4]Mucosal Immunology Unit, Laboratory of Parasitic Diseases; and [5]Lymphocyte Biology Section, Laboratory of Systems Biology; National Institute of Allergy and Infectious Diseases, NIH, Bethesda, MD 20892
[6]Immunology Graduate Group, University of Pennsylvania, Philadelphia, PA 19104
[7]Functional Genomics and Proteomics Facility, [8]Critical Care Medicine Department, Clinical Center, NIH, Bethesda, MD 20892
[9]Program in Metabolic Biology, Nutritional Science, and Toxicology, University of California, Berkley, Berkley, CA 94720

Dendritic cells (DCs) comprise distinct populations with specialized immune-regulatory functions. However, the environmental factors that determine the differentiation of these subsets remain poorly defined. Here, we report that retinoic acid (RA), a vitamin A derivative, controls the homeostasis of pre-DC (precursor of DC)–derived splenic CD11b$^+$CD8α^-Esam^{high} DCs and the developmentally related CD11b$^+$CD103$^+$ subset within the gut. Whereas mice deprived of RA signaling significantly lost both of these populations, neither pre-DC–derived CD11b$^-$CD8α^+ and CD11b$^-$CD103$^+$ nor monocyte-derived CD11b$^+$CD8α^-Esam^{low} or CD11b$^+$CD103$^-$ DC populations were deficient. In fate-tracking experiments, transfer of pre-DCs into RA-supplemented hosts resulted in near complete conversion of these cells into the CD11b$^+$CD8α^- subset, whereas transfer into vitamin A–deficient (VAD) hosts caused diversion to the CD11b$^-$CD8α^+ lineage. As vitamin A is an essential nutrient, we evaluated retinoid levels in mice and humans after radiation-induced mucosal injury and found this conditioning led to an acute VAD state. Consequently, radiation led to a selective loss of both RA-dependent DC subsets and impaired class II–restricted auto and antitumor immunity that could be rescued by supplemental RA. These findings establish a critical role for RA in regulating the homeostasis of pre-DC–derived DC subsets and have implications for the management of patients with immune deficiencies resulting from malnutrition and irradiation.

CORRESPONDENCE
Christopher A. Klebanoff:
klebanoc@mail.nih.gov
OR
Nicholas P. Restifo
restifo@nih.gov

Abbreviations used: ACT, adoptive T cell transfer; Ag, antigen; cDC, conventional DC; Ctrl, control; iLN, inguinal LN; pDC, plasmacytoid DC; RA, retinoic acid; RAR, RA receptor; RE, retinyl ester; rVV, recombinant vaccinia virus; RXR, retinoid X receptor; SILP, small intestine lamina propria; TBI, total body irradiation; VAD, vitamin A deficient.

All-trans–retinoic acid (RA), an activated metabolite derived from the essential nutrient vitamin A, plays a central role in embryonic and adult tissue development and homeostasis (Blomhoff and Blomhoff, 2006; Niederreither and Dollé, 2008; Napoli, 2012). By modulating transcriptional responses through activation of the ligand-induced RA receptors (RARs) and retinoid X receptors (RXRs), RA regulates pattern formation and terminal differentiation of pluripotent cells in organs as diverse as the central nervous, cardiovascular, limb, and genitourinary systems. Recently, RA's role in modulating tissue differentiation has been extended to include cells of the innate and adaptive immune systems where RA has been shown to serve a context-dependent regulatory function promoting either tolerance or immunity at

The Rockefeller University Press $30.00
J. Exp. Med. 2013 Vol. 210 No. 10 1961-1976
www.jem.org/cgi/doi/10.1084/jem.20122508

The Journal of Experimental Medicine

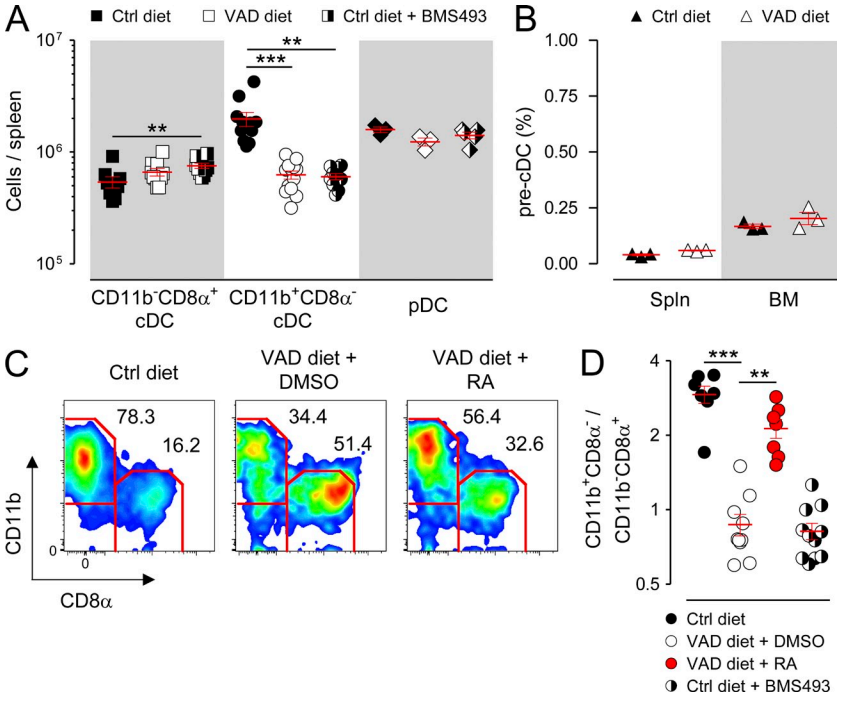

Figure 1. RA signaling controls splenic cDC composition. Mice fed either VAD or normal (Ctrl) diets were left untreated or received daily (i.p.) injections of either a pan-RAR antagonist (220 µg BMS493) or DMSO vehicle Ctrl. In addition, a subset of VAD mice were injected (i.p.) every 48 h with 250 µg exogenous RA or DMSO Ctrl for a total of three doses, with analysis performed on day 5. Spleens (Spln) and BM were then harvested and analyzed by flow cytometry. (A) Absolute numbers of splenic cDCs ($CD11c^{high}I\text{-}A/E^{+}$), including $CD11b^{-}CD8\alpha^{+}$ and $CD11b^{+}CD8\alpha^{-}$ subsets, and pDCs ($CD11c^{int}B220^{+}mPDCA1^{+}$) for the indicated groups; $n = 3$–13 mice per group. (B) Percentage of pre-cDCs ($lin^{-}CD11c^{high}I\text{-}A/E^{-}Flt3^{+}SIRP\alpha^{int}$) in the spleen and BM of Ctrl and VAD mice; $n = 3$ mice per group. (C) Splenocytes were gated on live, $CD11c^{high}I\text{-}A/E^{+}$ cells, and the percentages of splenic $CD11b^{+}CD8\alpha^{-}$ and $CD11b^{-}CD8\alpha^{+}$ cDCs in the indicated groups were assessed. A representative FACS plot from 7–11 independently evaluated mice per treatment group is shown. (D) Ratio of splenic $CD11b^{+}CD8\alpha^{-}/CD11b^{-}CD8\alpha^{+}$ cDCs for the indicated groups; $n = 7$–11 mice per group. All panels shown represent pooled data from two to four independently performed experiments. Horizontal bars indicate means ± SEM of individually evaluated mice. **, $P < 0.01$; ***, $P < 0.001$ (unpaired Student's *t* test).

mucosal surfaces (Mora et al., 2008; Hall et al., 2011b). For example, in the presence of transforming growth factor-β, RA signaling can significantly augment the expression of the lineage-specific transcription factor forkhead box P3 to generate suppressive extrathymic T regulatory cells (Benson et al., 2007; Coombes et al., 2007; Mucida et al., 2007; Sun et al., 2007). However, RA can also promote gut-associated immunity by serving as an obligate cofactor in the induction of IgA-producing B cells (Mora et al., 2006), IL-17–producing T helper cells (Hall et al., 2011a; Pino-Lagos et al., 2011), gut-tropic $CD4^{+}$ and $CD8^{+}$ T cells (Iwata et al., 2004; Benson et al., 2007; Sun et al., 2007; Hall et al., 2011a; Aoyama et al., 2013), IL-22–producing γδ T cells and innate lymphoid cells (Mielke et al., 2013), and proinflammatory conventional DCs (cDCs; DePaolo et al., 2011). In contrast, the function of RA in regulating systemic immunity is comparatively less well defined despite abundant epidemiological data implicating RA as a key factor in preventing and mitigating infectious diseases (Semba, 1999).

Here, we demonstrate that either acute or chronic deprivation of RA signaling, either through dietary or pharmacologic means, causes a selective loss in the pre-cDC (precursor of cDC)–derived splenic $CD11b^{+}CD8\alpha^{-}Esam^{high}$ cDC subset. Additionally, we found that the developmentally and genetically related orthologue of this cDC subset in the small intestine lamina propria (SILP), the $CD11b^{+}CD103^{+}$ population, is also dependent on RA to maintain its homeostasis. Moreover, we found that conditions that impair dietary absorption of essential nutrients, such as radiation-induced mucosal injury, cause an acute vitamin A–deficient (VAD) state in both humans and mice and a corresponding selective loss in the RA-dependent splenic $CD11b^{+}CD8\alpha^{-}Esam^{high}$ and SILP-associated $CD11b^{+}CD103^{+}$ cDCs. Mechanistically, these defects were not caused by a deficiency in the immediate hematopoietic progenitor of both cDC populations, the pre-cDCs, or an impaired proliferative or survival potential of mature cDC subsets. Rather, it resulted from a failure of the pre-cDCs to receive an RA-dependent differentiation prompt that controls the fate commitment of this cell between opposing cDC lineages. Collectively, these data provide new insight into environmental cues that instruct pre-cDCs to choose between alternative fates and further extend the critical role of RA in tuning immunity to include regulation of cDC composition within both central lymphoid and mucosal tissues.

RESULTS

RA signaling controls splenic cDC composition

To determine whether chronic vitamin A deficiency caused immune defects in a central lymphoid organ, we performed a comprehensive characterization of both innate and adaptive immune cell subsets in the spleens of mice maintained on a VAD diet compared with mice fed a control (Ctrl) diet. We found that VAD mice exhibited a significant loss in the absolute numbers of $CD11b^{+}CD8\alpha^{-}$ cDCs, the predominant DC present in the spleen under steady-state conditions which is specialized for class II–restricted antigen (Ag) presentation, relative to mice maintained on the Ctrl diet (Pooley et al., 2001; Dudziak et al., 2007; Kamphorst et al., 2010; Markey et al., 2012; Gatto et al., 2013). In contrast, VAD mice had preserved numbers of the two other major splenic DC subpopulations, the $CD11b^{-}CD8\alpha^{+}$ cDC and plasmacytoid DC

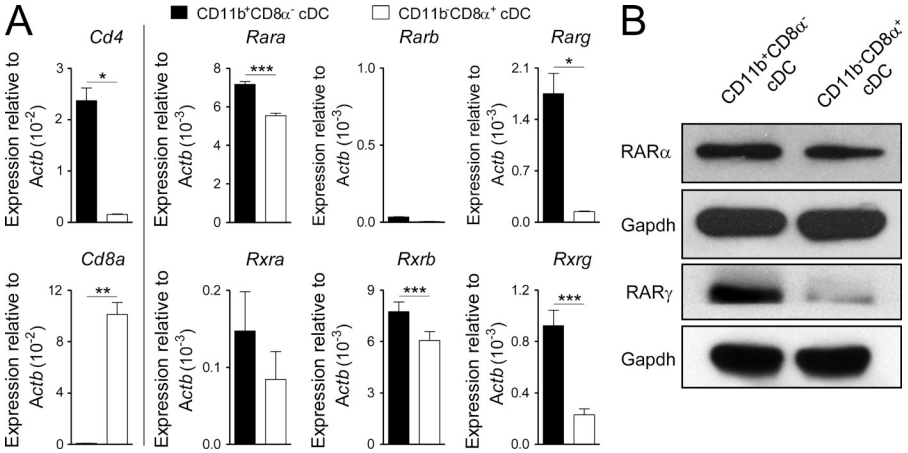

Figure 2. Retinoid and rexinoid receptor isoform expression in splenic cDC subsets. (A and B) Steady-state splenic CD11b$^+$CD8α$^-$ and CD11b$^-$CD8α$^+$ cDC (CD11c^{high}I-A/E$^+$) subsets were isolated by FACS sorting, and expression of retinoid and rexinoid receptor isoform expression was evaluated either by quantitative PCR (A) or Western blot analysis (B). Bars indicate means ± SEM. *, P < 0.05; **, P < 0.01; ***, P < 0.001 (unpaired Student's *t* test).

(pDC) subsets, which are specialized for Ag cross-presentation and type I interferon production, respectively (Fig. 1 A; den Haan et al., 2000; Dudziak et al., 2007; Belz and Nutt, 2012). The deficiency in CD11b$^+$CD8α$^-$ cDCs was not attributable to a loss in the frequency or absolute numbers of the immediate hematopoietic progenitor of cDCs, the pre-cDCs (Lin$^-$CD11c$^+$I-A/E$^-$Flt3$^+$SIRPα^{int}; Naik et al., 2006; Bogunovic et al., 2009; Ginhoux et al., 2009; Liu et al., 2009), in either the spleen or BM (Fig. 1 B and not depicted). Moreover, VAD mice possessed no significant numeric defects in conventional lymphoid subsets, including B, NK, and CD4$^+$ and CD8$^+$ T cells, compared with Ctrl mice (not depicted).

Because mice chronically deprived of vitamin A have multiple developmental defects (Blomhoff and Blomhoff, 2006), we also tested whether acute deprivation of RA signaling in Ctrl mice using BMS493, a pharmacologic antagonist for all three RAR isoforms (Germain et al., 2009), could phenocopy the splenic cDC defect observed in VAD mice. We found that a 9–10-d course of BMS493 administered by daily i.p. injection caused a significant loss in the absolute numbers of the CD11b$^+$CD8α$^-$ cDCs but not CD11b$^-$CD8α$^+$ cDCs, pDCs, or conventional lymphoid subsets, recapitulating the findings made in the VAD mice (Fig. 1 A). Consistent with earlier studies (Kuwata et al., 2000; Kastner et al., 2001), mice deprived of RA signaling exhibited a generalized expansion of macrophages and granulocytes in peripheral tissues (not depicted), suggesting that RA may serve a more general role in regulating the homeostasis of myeloid-derived cells.

As a consequence of the selective loss of CD11b$^+$CD8α$^-$ cDCs under conditions of RA signaling deprivation, whether through dietary or pharmacologic means, there was an inversion in the physiological ratio of the two splenic cDC populations (Fig. 1, C and D), leading to a predominance in the CD11b$^-$CD8α$^+$ subset. In the case of the VAD mice, this defect was partially rescued within 5 d by provision of exogenous RA (Fig. 1, C and D). These differences in the responsiveness of the CD11b$^+$CD8α$^-$ cDCs to RA signaling relative to the CD11b$^-$CD8α$^+$ subset correlated with systematic differences in RARα and RARγ receptor isoform expression from FACS-sorted cDC subsets (Fig. 2, A and B).

To evaluate whether an acute loss of RA signaling caused discernible defects in either the survival or propagation of mature splenic cDC subsets, we evaluated staining for the apoptosis marker annexin V and the proliferation marker Ki67 in cDC populations from Ctrl diet mice treated for 10 d either with vehicle Ctrl or BMS493. We found that in the setting of having an altered ratio of CD11b$^+$CD8α$^-$ to CD11b$^-$CD8α$^+$ cDCs (Fig. 3 A), there were no significant differences in either annexin V staining or Ki67 for a given subset in mice treated with BMS493 relative to those treated with the vehicle Ctrl (Fig. 3, B and C). We therefore conclude that either acute or chronic deprivation in RA signaling causes a selective loss in CD11b$^+$CD8α$^-$ cDCs in the spleen, leading to an inversion of the physiological balance between the CD11b$^+$CD8α$^-$ and CD11b$^-$CD8α$^+$ subsets. This defect was not attributable to a deficiency in the immediate hematopoietic progenitor of both cDC subtypes, the pre-cDC, nor the survival or proliferation of mature cDC subsets.

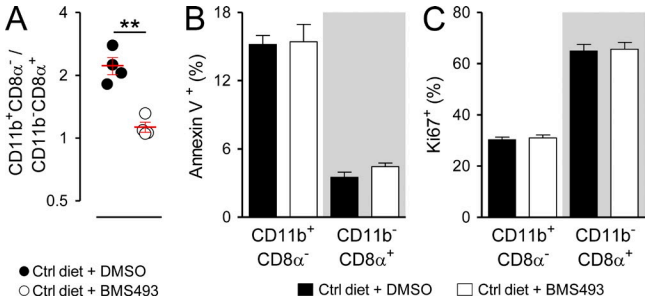

Figure 3. Acute deprivation of RA signaling alters splenic cDC composition without impacting subset proliferation or survival. Mice fed a normal (Ctrl) diet were injected (i.p.) daily for 10 d with a pan-RAR antagonist (220 µg BMS493) or DMSO vehicle Ctrl. Spleens from treated mice were then harvested and analyzed by flow cytometry by gating on live cDCs (CD11c^{high}I-A/E$^+$). (A–C) Scatter plot showing the ratio of splenic CD11b$^+$CD8α$^-$/CD11b$^-$CD8α$^+$ cDCs (A) and bar graphs demonstrating the frequency of either annexin V surface (B) or Ki67 intranuclear staining (C) in gated cDC subsets from Ctrl diet mice treated either with BMS493 or DMSO; *n* = 4 mice per group. Results from one of two representative experiments are shown. Bars indicate means ± SEM of individually evaluated mice. **, P < 0.01 (unpaired Student's *t* test).

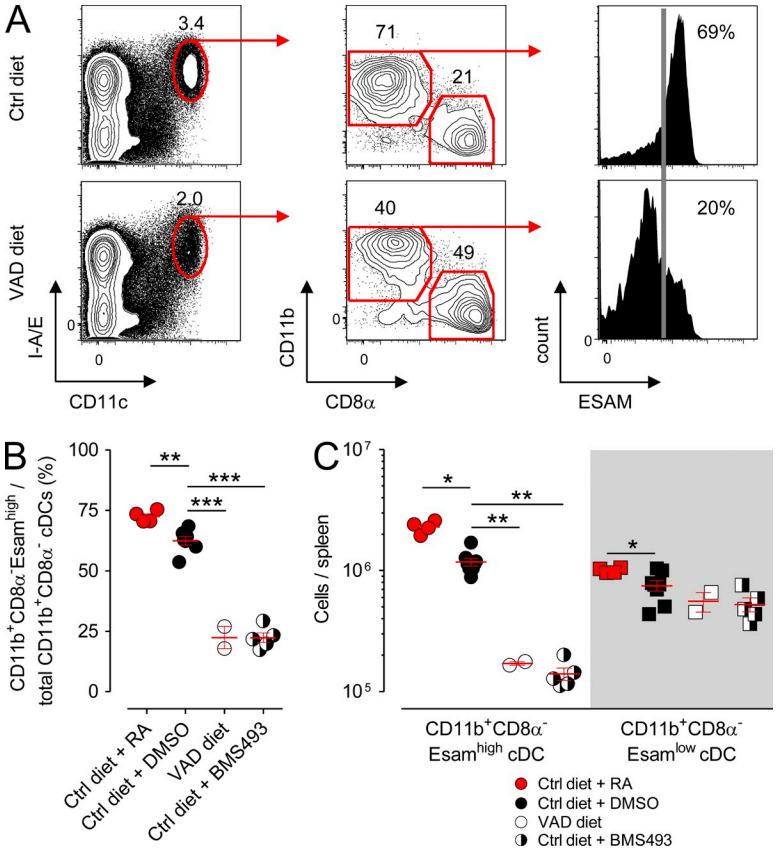

Figure 4. Deprivation of RA signaling causes a selective loss in the splenic CD11b$^+$CD8α$^-$Esam^{high} cDC population. Mice fed either VAD or normal (Ctrl) diets were left untreated or received daily (i.p.) injections of 250 µg RA, a pan-RAR antagonist (220 µg BMS493), or DMSO vehicle Ctrl. After 10 d, spleens from treated mice were harvested and analyzed by flow cytometry. (A) Representative FACS plots showing the gating strategy and frequency of splenic cDC (CD11c^{high}I-A/E$^+$) subsets, including the frequency of CD11b$^+$CD8α$^-$Esam^{high} cDCs, in mice maintained on either Ctrl or VAD diets. The frequency of Esam^{high} cells (vertical gray line) is based on isotype Ctrl staining. (B and C) Scatter plots showing the frequency of splenic CD11b$^+$Esam^{high} cDCs among all CD11b$^+$ cDCs (B) and absolute numbers of CD11b$^+$Esam^{high} and CD11b$^+$Esam^{low} cDCs from Ctrl diet, Ctrl diet + RA, VAD diet, or Ctrl mice treated with BMS493 (C); n = 2–7 mice per group. All panels shown are the pooled results of two independently performed experiments. Horizontal bars indicate means ± SEM of individually evaluated mice. *, P < 0.05; **, P < 0.01; ***, P < 0.001 (unpaired Student's t test).

Deprivation of RA signaling causes a selective loss in the splenic Esam^{high}CD11b$^+$ and SILP CD11b$^+$CD103$^+$ cDC subsets

Recently, Lewis et al. (2011) reported significant genetic, phenotypic, and functional heterogeneity within the splenic CD11b$^+$CD8α$^-$ cDC compartment discernible by the presence or absence of expression of Esam (endothelial cell–selective adhesion molecule), an immunoglobulin superfamily adhesion molecule. Whereas the CD11b$^+$Esam^{high} population identifies a Notch-dependent, pre-cDC–derived cDC subset that excels at CD4$^+$ T cell priming, the CD11b$^+$Esam^{low} population corresponds to a Notch-independent, monocyte-related cDC subset that possesses a superior capacity to release inflammatory cytokines such as TNF and IL-12. To determine whether deprivation of RA signaling impacted one or both of these splenic CD11b$^+$ cDC subsets, we evaluated the expression of Esam within the CD11b$^+$ cDC compartment in mice maintained on the Ctrl diet, VAD diet, or Ctrl diet in combination with BMS493. Consistent with the original description of the Esam-expressing splenic cDCs (Lewis et al., 2011), we found that roughly 70% of CD11b$^+$ cDCs in Ctrl diet mice also coexpressed high levels of this surface marker (Fig. 4 A). In VAD mice, there was a significant loss in the fractional percentage of CD11c^{high}I-A/E$^+$ cDCs attributable to a reduction in both the fractional percentage and absolute numbers of splenic CD11b$^+$CD8α$^-$Esam^{high} cDCs (Fig. 4, B and C). In contrast, the CD11b$^+$CD8α$^-$Esam^{low} population remained numerically unperturbed. These findings were recapitulated in mice acutely deprived of RA signaling using the pharmacologic antagonist BMS493. Conversely, provision of supplemental RA to mice maintained on the Ctrl diet caused a modest but significant increase in the percentage of CD11b$^+$CD8α$^-$Esam^{high} cDCs among the total CD11b$^+$ subset and also increased the absolute numbers of both the splenic CD11b$^+$Esam^{high} and CD11b$^+$Esam^{low} cDCs. Collectively, these data revealed that RA levels control the homeostasis of a specific pre-cDC–derived splenic cDC subset, the recently identified CD11b$^+$CD8α$^-$Esam^{high} population.

Outside of the spleen, tissue-specific factors are known to regulate the differentiation and composition of cDC subsets in organs such as the peripheral LNs and intestinal mucosa (Caton et al., 2007; Lewis et al., 2011; Gatto et al., 2013). We therefore next sought to determine whether RA was required for cDC development in these organs. Three phenotypically distinct cDC populations reside within the SILP of the gut, characterized in part by their expression pattern for the integrins CD11b and CD103: the CD11b$^+$CD103$^+$, CD11b$^-$CD103$^+$, and CD11b$^+$CD103$^-$ subsets (Sun et al., 2007; Bogunovic et al., 2009; Varol et al., 2009). Developmentally, the gut-associated CD11b$^+$CD103$^+$ and CD11b$^-$CD103$^+$ populations are analogous to the splenic CD11b$^+$CD8α$^-$Esam^{high} and CD11b$^-$CD8α$^+$ cDCs insofar as each of these subsets are derived from the progeny of pre-cDCs (Bogunovic et al., 2009; Varol et al., 2009; Satpathy et al., 2012). In contrast, mucosal CD11b$^+$CD103$^-$ cDCs, like the splenic CD11b$^+$

CD8α$^-$Esam^{low} subset, are of monocytic origin (Varol et al., 2007; Bogunovic et al., 2009;Varol et al., 2009; Satpathy et al., 2012). Moreover, recent bioinformatic analyses have demonstrated that the small intestine CD11b$^+$CD103$^+$ and CD11b$^-$CD103$^+$ cDC subsets are genetically orthologous to the splenic CD11b$^+$CD8α$^-$ and CD11b$^-$CD8α$^+$ cDC subsets, respectively, whereas the splenic CD11b$^+$CD8α$^-$Esam^{low} and mucosal CD11b$^+$CD103$^-$ populations cluster more closely to monocytes (Lewis et al., 2011; Miller et al., 2012). We found that deprivation of RA signaling in mice maintained on the VAD diet or the Ctrl diet treated with BMS493 exhibited a significant loss in both the fractional percentage and absolute numbers of the CD11b$^+$CD103$^+$ cDCs (Fig. 5, A–C). Reciprocally, we observed an increase in the pre-cDC–derived CD11b$^-$CD103$^+$ subset. These changes could be partially rescued by provision of a short course of exogenous RA. In contrast, the monocyte-derived CD11b$^+$CD103$^-$ population, like the splenic CD11b$^+$CD8α$^-$Esam^{low} subset, was not impacted by the presence or absence of RA signaling. In contrast, we found that neither the absolute numbers nor the ratio of tissue-resident CD11b$^+$CD8α$^-$ and CD11b$^-$CD8α$^+$ cDCs taken from inguinal LNs (iLNs) ofVAD mice were altered relative to that of Ctrl diet mice (Fig. 6, A–C). Collectively, we conclude that either acute or chronic deprivation in RA signaling causes a tissue-specific loss in the pre-cDC–derived splenic CD11b$^+$CD8α$^-$Esam^{high} and SILP-associated CD11b$^+$CD103$^+$ cDCs but not the monocyte-derived CD11b$^+$CD8α$^-$Esam^{low} nor the CD11b$^+$CD103$^-$ populations.

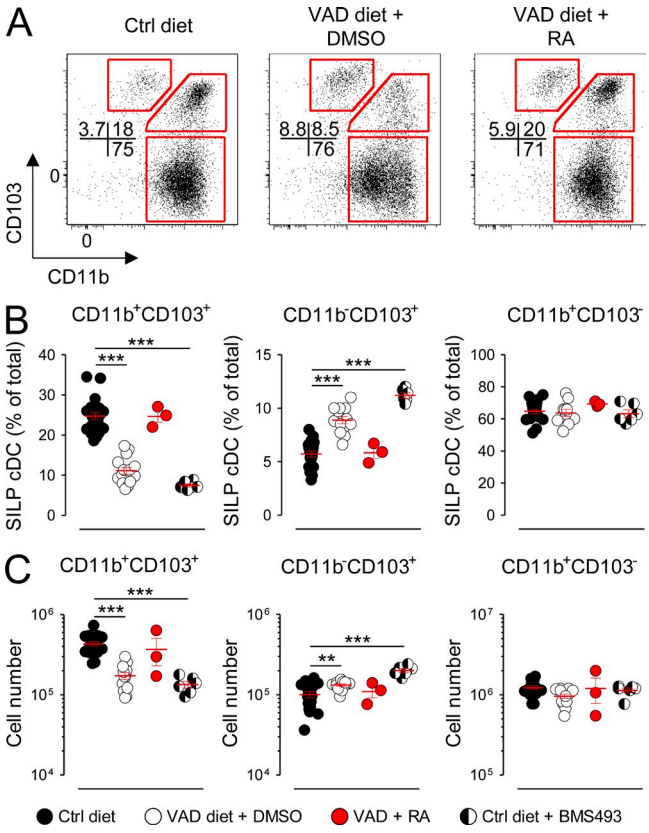

Figure 5. Deprivation of RA signaling causes a selective loss in the SILP CD11b$^+$CD103$^+$ cDC subset. Mice fed either VAD or normal (Ctrl) diets were left untreated treated or received daily (i.p.) injections of either a pan-RAR antagonist (220 µg BMS493) or DMSO vehicle Ctrl for 10 d. In addition, a subset of VAD mice were injected (i.p.) every 48 h with 250 µg exogenous RA or DMSO Ctrl for a total of three doses with analysis performed on day 5. Cells from the SILP were then harvested, and live gut-associated cDC (CD45$^-$CD11c^{high}I-A/E$^+$) subsets were analyzed by flow cytometry. (A–C) Representative FACS plots (A) and scatter plots showing either the fractional percentages (B) or absolute numbers (C) of SILP CD11b$^+$CD103$^+$, CD11b$^-$CD103$^+$, and CD11b$^+$CD103$^-$ cDC subsets from Ctrl diet, VAD diet, Ctrl diet + RA, or Ctrl mice + BMS493; n = 3–16 mice per group. All panels shown are the pooled results of at least two independently performed experiments. Horizontal bars indicate means ± SEM of individually evaluated mice. **, P < 0.01; ***, P < 0.001 (unpaired Student's t test).

Total body irradiation (TBI) induces an acute VAD state and a loss in RA-dependent cDC subsets

Higher animal species lack the capacity for de novo vitamin A synthesis. Consequently, vitamin A must be absorbed entirely through the diet to maintain physiological levels, a process which occurs primarily in the small intestine (Blomhoff and Blomhoff, 2006; Mora et al., 2008; Hall et al., 2011b). Because TBI, a component of standard preparative regimens used to facilitate autologous and allogeneic stem cell transplantations (Copelan, 2006) and experimental immunotherapies (Klebanoff et al., 2005; Dudley et al., 2008), causes significant injury to both the small and large intestines (Trier and Browning, 1966; Paulos et al., 2007), we next evaluated whether such conditioning could induce aVAD state in both humans and mice. We found that patients with metastatic melanoma receiving TBI as part of an autologous adoptive T cell transfer (ACT) immunotherapy (Dudley et al., 2008) developed a time-dependent loss in circulating levels of retinyl ester (RE), the primary form of vitamin A as it enters circulation after absorption from the gut (Fig. 7 A; Blomhoff and Blomhoff, 2006; Hall et al., 2011b). The degree of RE loss correlated with the magnitude of weight loss experienced by this cohort of patients, implying a relationship between the ability to absorb dietary-derived nutrients and vitamin A sufficiency (Fig. 7 B). These findings were confirmed in mice receiving TBI in which serum levels of both RE and RA itself were significantly depleted relative to nonirradiated Ctrls to a level comparable to that ofVAD diet hosts (Fig. 7 C).

To explore whether acute, irradiation-induced vitamin A deficiency led to changes in the composition of splenic cDCs, we performed immunotyping of spleen-derived cDC subsets 10 d after TBI. Consistent with the phenotypes of both the VAD diet and RAR inhibitor–treated mice, we found that TBI resulted in a loss in the fractional percentage of splenic CD11b$^+$CD8α$^-$ relative to CD11b$^-$CD8α$^+$ cDCs (Fig. 7 D). Provision of exogenous RA (Fig. 7, D and E) or a synthetic RARα-specific agonist (not depicted) restored the physiological ratio of CD11b$^+$CD8α$^-$ to CD11b$^-$CD8α$^+$ cDCs, confirming that the cDC defect observed in irradiated hosts was caused by an acquired RA deficiency. Finally, we evaluated

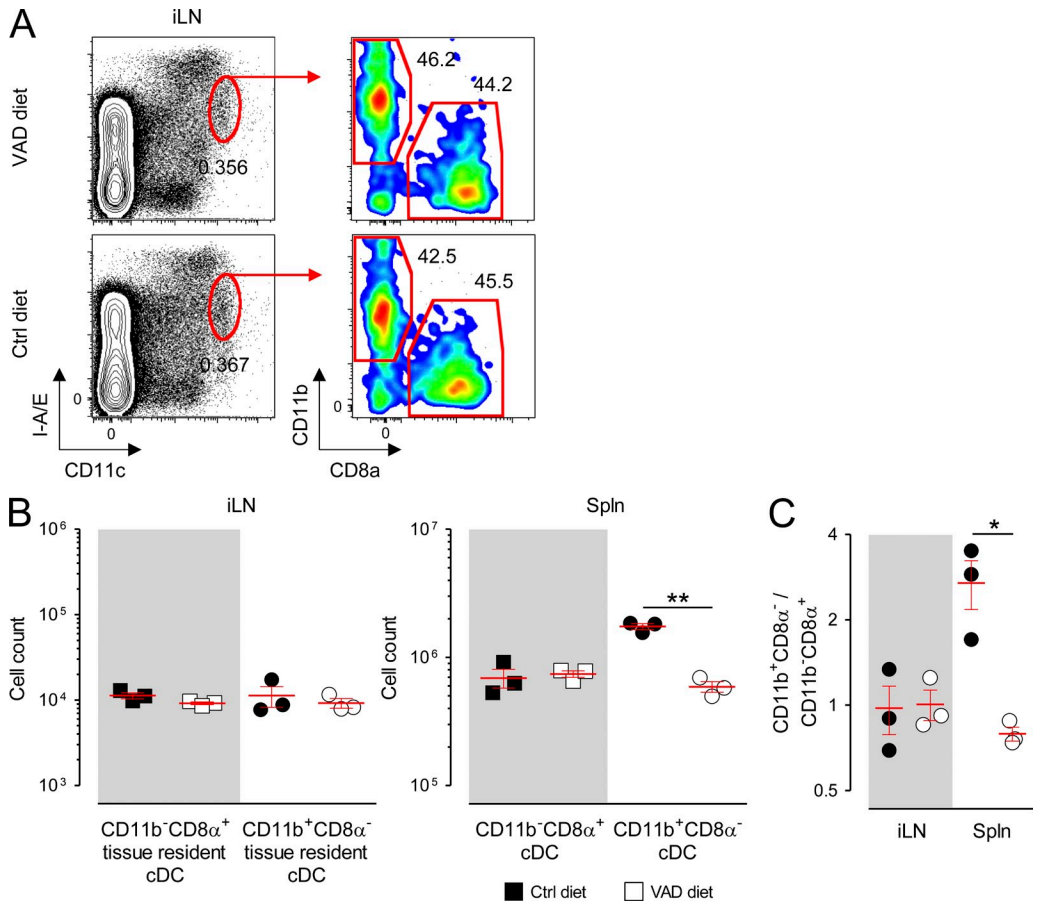

Figure 6. RA controls the homeostasis of tissue-resident cDC subsets in a tissue-specific manner. Mice were fed either VAD or normal (Ctrl) diets and spleens (Spln) and iLNs from these mice were harvested and analyzed by flow cytometry. (A) Representative FACS plots showing the gating strategy and fractional percentage of tissue-resident cDC (CD11c^{high}I-A/E^{int}) CD11b$^+$CD8α$^-$ and CD11b$^-$CD8α$^+$ subsets from the iLNs of VAD and Ctrl diet mice. (B and C) Scatter plots showing the absolute numbers (B) and ratios of tissue-resident CD11b$^+$CD8α$^-$ to CD11b$^-$CD8α$^+$ cDC subsets (C) in the iLNs and Splns of VAD and Ctrl diet mice; $n = 3$ mice per group. Data shown represent the pooled results of two independently performed experiments. Horizontal bars indicate means ± SEM of individually evaluated mice. *, $P < 0.05$; **, $P < 0.01$ (unpaired Student's t test).

the absolute numbers of splenic cDC subsets after TBI in mice treated with ACT. As previously reported, TBI caused an acute loss in multiple hematologic cell types, including both splenic cDC subsets (Zhang et al., 2002). However, although CD11b$^-$CD8α$^+$ cDCs reconstituted spontaneously 2 wk after TBI conditioning, the CD11b$^+$CD8α$^-$ cDC subset did not rise above their nadir unless exogenous RA was provided (Fig. 7 F).

Earlier, we demonstrated that deprivation of RA signaling either by dietary or pharmacologic means caused a selective depletion of a specific subset of splenic CD11b$^+$ cDCs identified through the coexpression of the surface molecule Esam. To determine whether TBI-induced vitamin A depletion also resulted in a defect in the CD11b$^+$CD8α$^-$Esam^{high} population, we administered titrated doses of TBI to mice to produce a graded deficiency in the circulating retinoids RE and RA (Fig. 8, A and B) and evaluated the composition of splenic cDCs 10 d later. We observed that irradiation caused a dose-dependent loss in the CD11b$^+$CD8α$^-$Esam^{high} population (Fig. 8, C and D). Moreover, we found that the loss in the fractional percentage of this population significantly correlated with contemporaneously evaluated values of serum RE (Fig. 8 E). Finally, we evaluated the complement of cDC subsets in the SILP of mice who received 6 Gy TBI or sham treatment. Similar to findings made in the spleen, we found that irradiation caused a selective deficiency in the absolute numbers of the RA-dependent CD11b$^+$CD103$^+$ subset but neither the CD11b$^-$CD103$^+$ nor CD11b$^+$CD103$^-$ populations (Fig. 8, F and G). We therefore conclude that TBI induces an acute vitamin A–depleted state in both humans and mice. Correlated with this state and recapitulating findings made in mice deprived of RA signaling by dietary or pharmacologic means, we found that irradiated mice exhibit a selective deficiency in the RA-dependent splenic CD11b$^+$CD8α$^-$Esam^{high} and SILP-associated CD11b$^+$CD103$^+$ cDCs.

Relative levels of RA signaling dictate pre-cDC commitment between opposing cDC subsets

To gain greater insight into the mechanism by which RA influences splenic cDC composition, we FACS sorted naturally

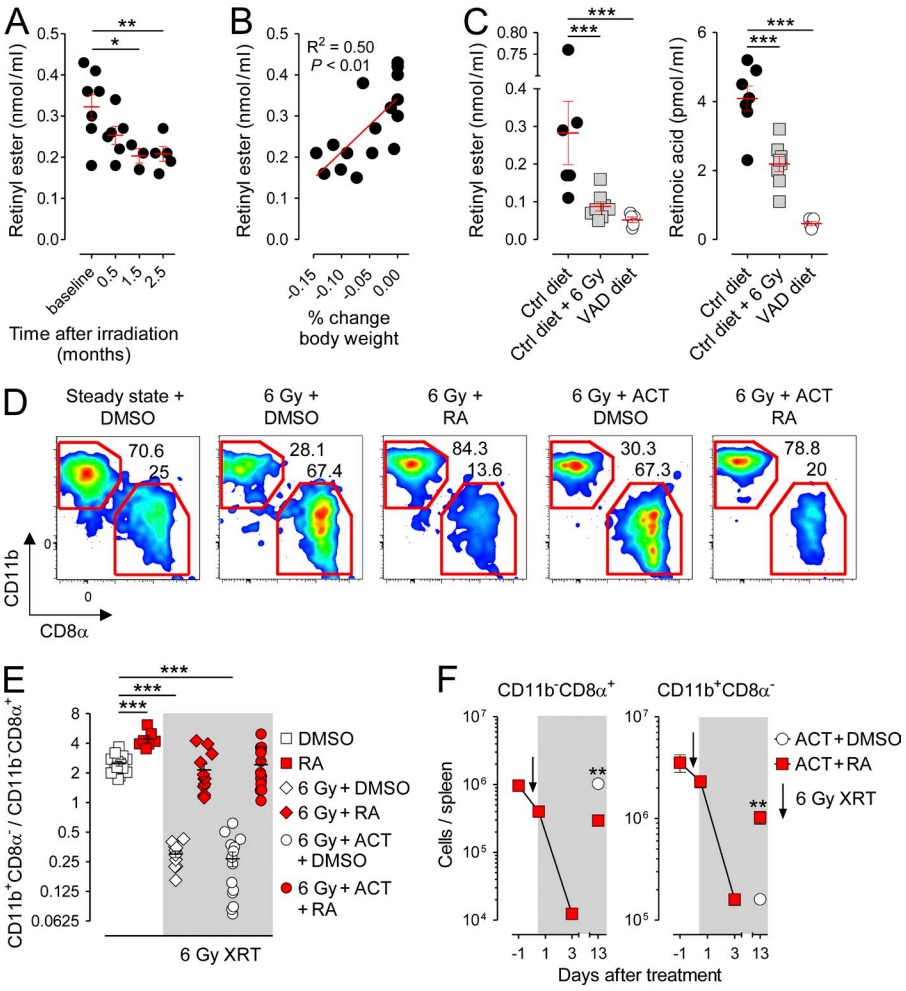

Figure 7. TBI induces an acute vitamin A–depleted state in humans and mice and a reversible loss in splenic CD11b⁺CD8α⁻ cDCs. Patients with metastatic cutaneous melanoma and mice maintained on a normal (Ctrl) diet bearing B16 melanoma tumors received blood draws before and after TBI. (A and B) Quantification of serum RE levels (A) and correlation of serum RE levels with fractional changes in body weight (B) in patients with metastatic melanoma before and after receiving TBI conditioning for autologous ACT immunotherapy; $n = 3$–8 patients/time point. (C) Quantification of serum RE and RA levels in Ctrl diet tumor-bearing mice 10 d after receiving sham treatment or TBI and non-irradiated VAD diet mice; $n = 5$–8 mice per treatment condition. (D and E) Representative FACS plots showing splenic cDC (CD11c^{high}I-A/E⁺) CD11b⁺CD8α⁻ and CD11b⁻CD8α⁺ subsets (D) and scatter plot showing the ratio of CD11b⁺CD8α⁻/CD11b⁻CD8α⁺ splenic cDCs in Ctrl diet mice 10 d after receiving TBI or sham treatment and exogenous RA or DMSO with or without ACT (E); $n = 7$–15. (F) Absolute numbers of CD11b⁺CD8α⁻ and CD11b⁻CD8α⁺ splenic cDCs after TBI conditioning and ACT treated with exogenous RA or DMSO; $n = 3$ mice per data point. All data shown are representative of at least two independently performed experiments. Horizontal bars indicate means ± SEM of individually evaluated mice. *, $P < 0.05$; **, $P < 0.01$; ***, $P < 0.001$ (unpaired Student's *t* test).

occurring CD11b⁺CD8α⁻ and CD11b⁻CD8α⁺ cDCs that had reconstituted in vivo in TBI-conditioned, acutely VAD mice provided either DMSO vehicle Ctrl or exogenous RA. From these sorted cDC subsets, we performed whole transcriptome analysis. Consistent with the cDC phenotype of both the VAD hosts and mice receiving TBI, we found that the CD11b⁺CD8α⁻ population demonstrated greater gene responsiveness to RA exposure in vivo, as measured by the number of unique genes significantly regulated up or down, relative to the CD11b⁻CD8α⁺ subset (273 vs. 144 genes; false discovery rate $P < 0.01$; Table S1). In both subsets, transcripts for established target genes of RA signaling, such as *Mmp9*, *Aldh1a2*, *Itgae*, and *Tgm2* (Blomhoff and Blomhoff, 2006), were significantly up-regulated with RA exposure, confirming the activity of the exogenously administered vitamin (Fig. 9 A). Notably, although the CD11b⁺CD8α⁻ subset requires signaling through the LTβR (lymphotoxin β receptor) for its homeostasis (Kabashima et al., 2005; Lewis et al., 2011), we did not observe dynamic changes in the expression of RelB-dependent downstream targets of LTβR signaling, such as *Ccl19*, *Ccl21*, *Cxcl12* (a.k.a. SDF-1a), *Cxcl13*, and *Tnfsf13b* (a.k.a. BAFF; Wu et al., 1998; Dejardin et al., 2002), with RA treatment in either subset (not depicted).

In Fig. 8, we showed that deprivation of RA signaling through TBI conditioning caused a selective loss in the splenic CD11b⁺CD8α⁻Esam^{high} cDC subset. To determine whether the loss in this subpopulation was evident genetically, we next compared our microarray data with a group of signature genes reported by Lewis et al. (2011) to be highly enriched in either the Esam^{high} or Esam^{low} populations (Fig. 9 B). Consistent with the phenotype of the remaining CD11b⁺ cDCs that reconstituted in irradiated mice, we found that monocyte-specific genes characteristic of the Esam^{low} population, such as *Ly6c*, *Lyz2*, *Csf1r*, and *Ccr2*, predominated. In contrast, the CD11b⁺CD8α⁻ cDCs that reconstituted in irradiated mice rescued with exogenous RA expressed Esam^{high} signature genes such as *Esam* itself and the G protein–coupled receptor *Gpr4*. Overall, we found a highly significant ($P < 0.001$) association between the Esam^{high} versus Esam^{low} gene signature reported by Lewis et al. (2011) and the gene expression pattern of the CD11b⁺CD8α⁻ cDCs that reconstituted in irradiated mice given RA versus vehicle Ctrl. Only the expression of 2 out of 18 signature genes, *Tlr11* and *Dtx1*, were discordant between datasets. Together, these data provide further evidence that the RA-dependent, pre-cDC–derived CD11b⁺CD8α⁻Esam^{high} cDC

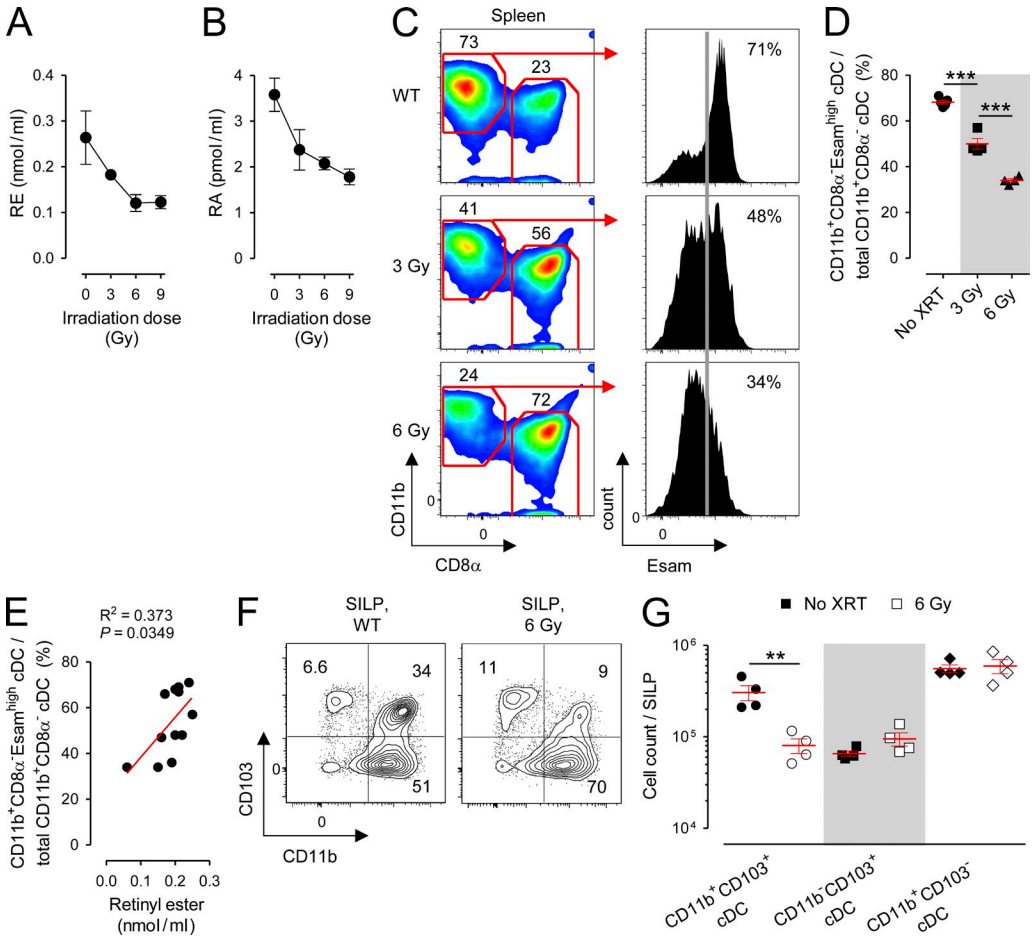

Figure 8. TBI causes a dose-dependent reduction in circulating retinoids and a loss of RA-dependent cDC subsets in the spleen and gut. Mice maintained on a normal (Ctrl) diet were left untreated as Ctrls or received titrated doses of TBI, and blood, spleens, and cells isolated from the SILP were collected for analysis. (A and B) Serum measurements of RE (A) and RA (B) in Ctrl diet mice 10 d after receiving the indicated doses of TBI; $n = 4$–13 mice per condition. (C and D) Representative FACS plots (C) and scatter plot (D) showing the percentage of splenic CD11b$^+$CD8α$^-$Esam^{high} cDCs (CD11c^{high}I-A/E$^+$) among all CD11b$^+$CD8α$^-$ cDCs in mice maintained on a Ctrl diet who received either sham treatment or titrated doses of TBI 10 d prior; $n = 4$ mice per group. The frequency of Esam^{high} cells (vertical gray line) is based on isotype Ctrl staining. (E) Linear regression analysis of the fractional percentage of splenic CD11b$^+$CD8α$^-$Esam^{high} cDCs among total CD11b$^+$CD8α$^-$ cDCs as a function of serum RE values in mice who received titrated doses of TBI. (F and G) Representative FACS plots (F) and absolute numbers (G) of SILP cDC subsets in mice maintained on a Ctrl diet who received either sham treatment or 6 Gy of TBI 10 d prior; $n = 4$ mice per group. All data shown are representative of two independently performed experiments. Horizontal bars indicate means ± SEM of individually evaluated mice. **, $P < 0.01$; ***, $P < 0.001$ (unpaired Student's t test).

subset is lost in the setting of TBI conditioning, leaving the monocyte-derived CD11b$^+$CD8α$^-$Esam^{low} population as the remaining CD11b$^+$ cDC population.

We next evaluated genes uniquely modulated by RA exposure in the CD11b$^+$CD8α$^-$ but not the CD11b$^-$CD8α$^+$ cDC subset. Surprisingly, we found that genes encoding key lineage-associated transcription factors, C-type lectins, and other surface molecules associated with CD11b$^-$CD8α$^+$ cDCs, including *Irf8*, *Clec9a*, *CD36*, *Tlr3*, and even *CD8a* itself, were all significantly and uniquely down-regulated in CD11b$^+$CD8α$^-$ cDCs upon RA exposure in vivo (Fig. 9 C). These findings, combined with our observations that pre-cDCs were numerically unaffected by vitamin A deficiency and that RA signaling did not impact either the survival or proliferation of mature cDC subsets, led us to postulate that relative levels of RA signaling may influence the in vivo fate commitment of pre-cDCs in vivo.

To test this hypothesis, we adoptively transferred congenically distinguishable Ly5.2$^+$ BM-derived pre-cDCs FACS sorted to >96% purity into nonirradiated Ly5.1$^+$ hosts and evaluated the composition of pre-cDC progeny in the spleen 6–7 d after transfer (Fig. 9, D and E). To evaluate the influence of RA signaling on the in vivo fate commitment of pre-cDCs, we transferred pre-cDCs into recipient mice maintained on a VAD or Ctrl diet in combination with either exogenous RA or BMS493. Consistent with earlier studies (Naik et al., 2006; Liu et al., 2009), the vast majority of progeny cells derived from pre-cDCs were CD11c$^+$I-A/E$^+$, confirming their restricted lineage potential to become cDCs (Fig. 9 E). Moreover, as had also been previously demonstrated (Liu et al., 2009),

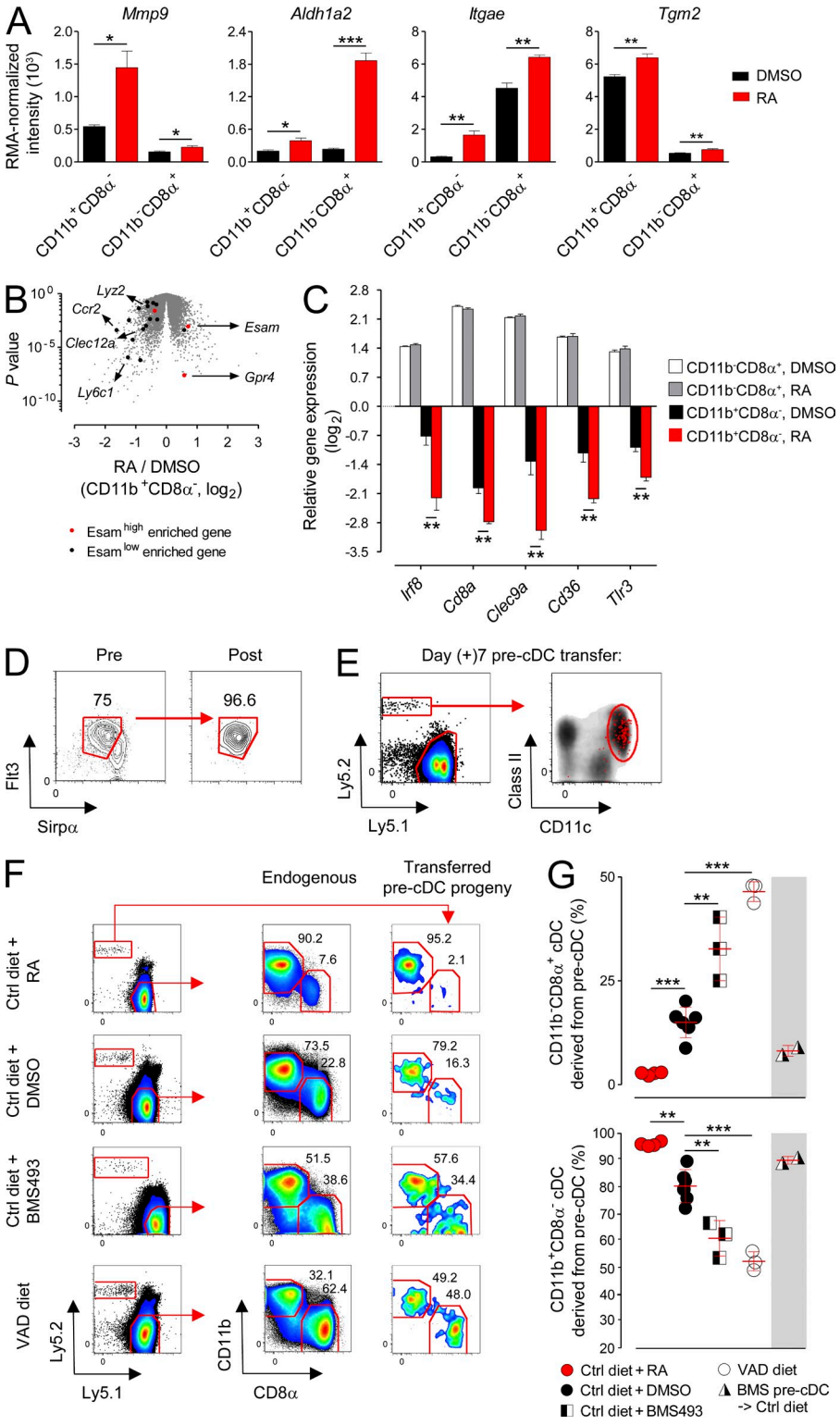

Figure 9. Relative levels of RA signaling determine the in vivo fate commitment of splenic pre-cDCs. (A) Normalized expression values of transcripts for established RA-responsive target genes in FACS-sorted splenic cDC ($CD11c^{high}$I-A/E$^+$) subsets treated in vivo for 7 d with daily i.p. injections of RA or DMSO Ctrl during reconstitution after 6 Gy TBI conditioning; $n = 4$ biological replicates per condition. (B) Volcano plot comparing p-value versus fold change for microarray probes from FACS-sorted $CD11b^+CD8\alpha^-$ cDCs reconstituted in vivo in mice treated with TBI conditioning and exogenous RA or DMSO Ctrl. Genes enriched in the $CD11b^+CD8\alpha^-Esam^{high}$ and $C11b^+CD8\alpha^-Esam^{low}$ cDC subsets, as reported by Lewis et al. (2011), are highlighted in red and black, respectively. Some characteristic genes are indicated. $P < 0.001$ (χ^2 test). (C) The ratio of expression ($\log_2$ scale) of selected genes uniquely regulated by RA in vivo in the $CD11b^+CD8\alpha^-$ but not $CD11b^-CD8\alpha^+$ splenic cDC subset. (D and E) Isolation by FACS sorting (D) and splenic progeny of BM-derived Ly5.2$^+$ pre-cDCs 7d after transfer into congenically distinguishable Ly5.1$^+$ nonirradiated host mice (E). FACS plots are shown after gating on viable cells with back-gated Ly5.2$^+$ cells shown in red. (F and G) Representative FACS plots (F) and scatter plot (G) showing the composition of Ly5.2$^+$ pre-cDC–derived progeny and endogenous cDC subsets in the spleens of nonirradiated Ly5.1$^+$ host mice maintained on a normal (Ctrl) diet, Ctrl diet + RA, Ctrl diet + BMS493, or VAD diet; $n = 3$–6 mice per treatment group. FACS plots demonstrating the distribution of endogenous cDC subsets and the progeny of transferred pre-cDCs are shown after gating on viable $CD11c^+$I-A/E$^+$ cells. Where indicated, donor mice were pretreated with BMS493 for 10 d before pre-cDC collection. Bars indicate means ± SEM of individually evaluated mice. All data shown are representative of two to four independently performed experiments. *, $P < 0.05$; **, $P < 0.01$; ***, $P < 0.001$ (unpaired Student's t test).

the subset distribution of cDCs after pre-cDC adoptive transfer into Ctrl diet hosts did not precisely recapitulate the endogenous balance, with an even greater bias toward the $CD11b^+CD8\alpha^-$ subset than is physiologically observed (Fig. 9 F). We found that administration of supplemental RA to mice maintained on a Ctrl diet almost quantitatively induced the differentiation of pre-cDC progeny into $CD11b^+CD8\alpha^-$ cDCs while limiting the formation of $CD11b^-CD8\alpha^+$ cDCs (Fig. 9, F and G). Conversely, transfer of pre-cDCs into Ctrl diet mice administered BMS493 or mice maintained on the

VAD diet led to a significant enrichment in the CD11b$^-$CD8α$^+$ cDC subset relative to Ctrl mice (Fig. 9, F and G). Relative levels of RA did not impact pre-cDC engraftment as the recovery of pre-cDC progeny was similar across all hosts tested (not depicted).

To evaluate at what stage in pre-cDC development RA signaling influenced their capacity to form alternative cDC subsets, we isolated cells from mice treated for 10 d with BMS493. After confirming the in vivo activity of BMS493 in donor mice by measuring an altered splenic CD11b$^+$CD8α$^-$/CD11b$^-$CD8α$^+$ ratio (not depicted), we transferred these BMS493 conditioned pre-cDCs into Ctrl diet mice and evaluated the distribution of their cDC progeny. In contrast with results obtained when pre-cDCs derived from Ctrl diet donor mice were transferred into BMS493-treated or VAD hosts, we found that pre-cDCs taken from BMS493-conditioned mice were not significantly impaired in their ability to form the CD11b$^+$CD8α$^-$ subset relative to pre-cDCs obtained from donor mice not deprived of RA signaling (Fig. 9 G). Collectively, we conclude that relative levels of RA signaling determine the in vivo fate commitment of splenic pre-cDCs between alternative cDC subsets such that under conditions of RA sufficiency, the progeny become predominantly CD11b$^+$CD8α$^-$ cDCs, whereas under conditions of RA signaling deprivation, a greater proportion differentiates into the CD11b$^-$CD8α$^+$ population.

RA enhances class II–restricted auto and antitumor immunity in mice rendered VAD through TBI conditioning

Mucosal injury after TBI conditioning for hematopoietic cell transplantation has been correlated with the acquisition of an immune-deficient state with systemic consequences. Functionally, this state includes a selective loss in the absolute numbers and class II–restricted Ag presentation capacity of the splenic CD11b$^+$CD8α$^-$ cDC subset (Markey et al., 2012). We sought to ascertain whether the selective deficiencies in the splenic CD11b$^+$CD8α$^-$Esam^{high} and SILP-associated CD11b$^+$CD103$^+$ cDC subsets in the setting of acute vitamin A deficiency caused by TBI conditioning had an immunological impact on systemic cDC-dependent T cell immunity. Therefore, we transferred either Trp-1 or Pmel-1 CD4$^+$ and CD8$^+$ T cells, which recognize the shared melanocyte/melanoma differentiation Ags tyrosinase and gp100 in a class II– and class I–restricted fashion, respectively, into mice bearing established s.c. B16 melanoma tumors treated with TBI conditioning before T cell infusion and assessed for ocular autoimmunity and tumor regression. In addition to T cells, treated mice also received concurrent vaccination with a recombinant vaccinia virus (rVV) encoding cognate Ag and IL-2.

Optimal induction of tumor regression and autoimmunity in both the Trp-1 and Pmel-1 model systems are vaccine dependent (Overwijk et al., 2003; Muranski et al., 2008). We found that the full expansion of CD4$^+$ and CD8$^+$ T cells in response to rVV vaccination was dependent on an intact CD11c$^+$ Ag-presenting cell population as cDC depletion using the CD11c-DTR system significantly impaired the expansion of both Trp-1 CD4$^+$ and Pmel-1 CD8$^+$ T cells (Fig. 10, A and B). To determine the relative contributions of the splenic CD11b$^+$CD8α$^-$ and CD11b$^-$CD8α$^+$ cDC subsets on vaccine-induced priming in our model systems, we FACS sorted each subset 36 h after systemic vaccination with rVV and probed the ability of these subsets to induce activation and CFSE dilution of naive Trp-1 CD4$^+$ and Pmel-1 CD8$^+$ T cells ex vivo. Consistent with studies using the OVA model Ag to prime naive T cells in vivo (Dudziak et al., 2007; Lewis et al., 2011; Gatto et al., 2013), we found that the isolated CD11b$^+$CD8α$^-$ cDC population was far more efficient at priming naive CD4$^+$ T cell relative to the CD11b$^-$CD8α$^+$ cDC subset across a range of T cell to cDC ratios (Fig. 10, C and D). In contrast, CD11b$^-$CD8α$^+$ cDCs were uniquely able to cross present and activate naive Pmel-1 CD8$^+$ T cells. These findings were confirmed in vivo by demonstrating that the full proliferation of naive OT-II CD4$^+$ TCR transgenic T cells in response to full-length OVA protein vaccination was impaired in mice acutely depleted of the splenic CD11b$^+$CD8α$^-$Esam^{high} and SILP-associated CD11b$^+$CD103$^+$ cDC subsets using BMS493 (not depicted).

When self/tumor-reactive T cells were transferred into mice rendered acutely VAD through TBI conditioning followed by rVV vaccination, we found that provision of exogenous RA significantly augmented both ocular autoimmunity (Fig. 10 E) and tumor immunity (Fig. 10 F) mediated by CD4$^+$ T cells but not CD8$^+$ T cells. Notably, RA administration alone had no impact on the kinetics of tumor growth. We conclude that provision of exogenous RA to mice rendered acutely VAD through TBI conditioning enhances class II– but not class I–restricted auto and antitumor immunity, correlating with the reconstitution of the CD11b$^+$CD8α$^-$ cDC subset, which possesses a superior ability to stimulate CD4$^+$ T cells.

DISCUSSION

The cascade of progressively lineage-restricted hematopoietic progenitors leading to the formation of cDCs has substantially been resolved (Merad et al., 2013), including the recent identification of pre-cDCs as the immediate precursor of tissue-resident cDCs in both lymphoid (Naik et al., 2006; Liu et al., 2009) and nonlymphoid peripheral tissues (Bogunovic et al., 2009; Ginhoux et al., 2009; Varol et al., 2009). However, the local environmental factors that regulate the final differentiation step of pre-cDCs between two functionally, anatomically, and genetically distinct subsets has remained unclear. Our data demonstrate that signaling mediated by RA, an activated form of the essential nutrient vitamin A, plays a critical role in maintaining the homeostasis of both the splenic CD11b$^+$CD8α$^-$Esam^{high} cDC and its related counterpart within the SILP, the CD11b$^+$CD103$^+$ subset. Under conditions of RA signaling deprivation, whether through the chronic administration of a VAD diet or acutely through administration of a pan-RA antagonist or exposure to TBI, we observed a selective and RA-reversible defect in both of these subsets. In contrast, no deficiency in the pre-cDC–derived splenic CD11b$^-$CD8α$^+$ and gut-associated CD11b$^-$CD103$^+$ cDCs

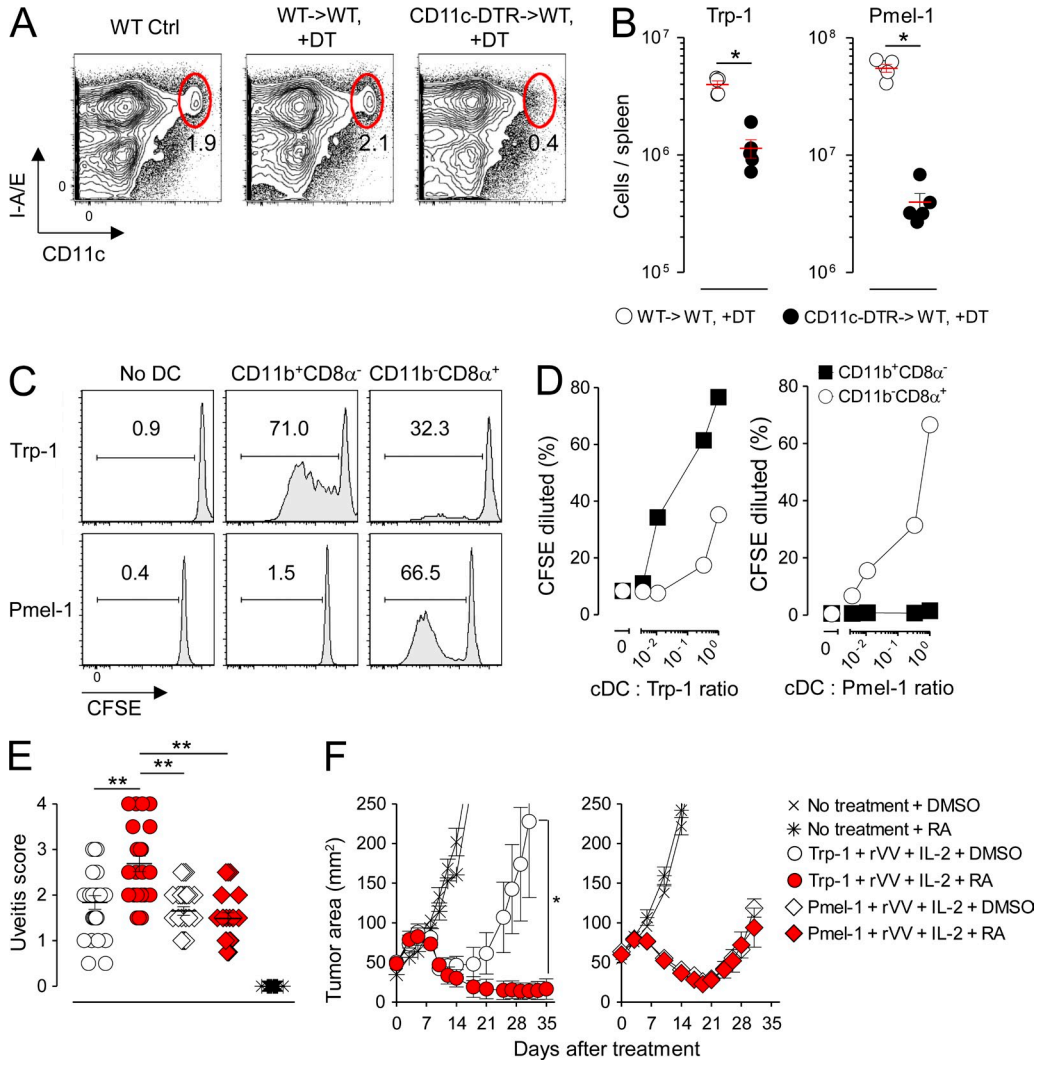

Figure 10. RA selectively augments MHC class II– but not class I–restricted autoimmunity and antitumor immunity in mice rendered acutely VAD through TBI conditioning. Lethally irradiated (9 Gy) mice were reconstituted either with WT BM (WT→WT) or BM derived from CD11c–diphtheria toxin receptor mice (CD11c-DTR→WT). After reconstitution, radiation chimeras were treated with diphtheria toxin (DT), and 10^6 naive Trp-1 $CD4^+$ T cells or Pmel-1 $CD8^+$ T cells were adoptively transferred in combination with 2×10^7 PFU of an rVV encoding cognate Ag for the transferred T cells. (A and B) Representative FACS plots showing depletion of splenic cDCs ($CD11c^{high}$I-A/E^+; A) and scatter plots showing the absolute number of transferred Trp-1 $CD4^+$ T cells or Pmel-1 $CD8^+$ T cells in the spleen at the peak (day 5) of the immune response after vaccination (B); $n = 4$ mice per group. This experiment was repeated twice with similar results. (C and D) Representative FACS plots showing the proliferation of naive, Ly5.2$^+$ CFSE-labeled Trp-1 $CD4^+$ or Pmel-1 $CD8^+$ T cells in response to stimulation with FACS-sorted Ly5.1$^+$ splenic $CD11b^+CD8\alpha^-$ and $CD11b^-CD8\alpha^+$ cDC subsets isolated 36 h after in vivo vaccination with rVV at a 1:1 ratio (C) or at titrated cDC/T cell ratios (D). CFSE proliferation was measured on day 5 after stimulation after gating on live$^+$, singlet$^+$, Ly5.1$^-$, Ly.5.2$^+$, $CD3^+CD4^+$, or $CD3^+CD8^+$ cells. Data shown are representative of two independently performed experiments. (E) Ocular autoimmune pathology scores 14 d after mice were rendered acutely VAD in response to TBI conditioning followed by treatment with exogenous RA or DMSO Ctrl administered alone or in combination with transfer of 10^6 Trp-1 $CD4^+$ or Pmel-1 $CD8^+$ T cells. Pooled results from two independently performed experiments are shown; $n = 20$–30 evaluated eyes per treatment group. Horizontal bars indicate means ± SEM of individually evaluated eyes. *, $P < 0.05$; **, $P < 0.01$ (unpaired Student's t test). (F) Treatment of 10-d established s.c. B16 melanoma tumors in mice rendered acutely VAD in response to TBI conditioning treated with exogenous RA or DMSO Ctrl administered alone or in combination with transfer of 10^6 Trp-1 $CD4^+$ or Pmel-1 $CD8^+$ T cells; $n = 5$ mice per treatment group. Data shown are representative of three independently performed tumor treatment experiments. Horizontal bars indicate means ± SEM of individually evaluated mice. *, $P < 0.05$ (Wilcoxon rank sum). All mice treated in E and F received concurrent vaccination with rVV and exogenous IL-2.

was appreciated, nor was there a defect in the monocyte-derived $CD11b^+CD8\alpha^-Esam^{low}$ and $CD11b^+CD103^-$ subsets. The finding that RA regulates the homeostasis of the splenic $CD11b^+CD8\alpha^-Esam^{high}$ cDCs was recently confirmed in a separate manuscript by Beijer et al. (2013). Mechanistically, we found no evidence of a numeric pre-cDC defect in either the BM or spleen in VAD mice, nor did we observe any defects in survival or proliferation markers in mature cDC subsets

acutely deprived of RA signaling. Rather, we found that relative levels of RA signaling were deterministic in influencing the pre-cDCs commitment between alternative subsets.

Vitamin A can have pleotropic effects on many cells throughout the body, particularly with chronic vitamin A deficiency present in aged mice maintained on a VAD diet. For this reason, we made use of two additional experimental modalities to induce an acute vitamin A deficiency and confirm our findings made in mice maintained on the VAD diet. Specifically, we acutely deprived mice of RA signaling either through acute pharmacologic deprivation using the pan-RAR antagonist BMS493 or through induction of an acute VAD state through TBI. Although each of these approaches has their own potential for confounding variables, all three approaches gave the same experimental result: a selective loss in the splenic $CD11b^+CD8\alpha^-Esam^{high}$ and gut-associated $CD11b^+CD103^+$ cDC subsets. Moreover, provision of a short course of RA to either VAD mice over 5–7 d to rescue the cDC phenotype in these mice provided an additional specificity Ctrl as this intervention rescued the splenic and gut cDC phenotypes. Finally, by transferring the pre-cDCs, a highly purified and phenotypically well-defined cell population, into vitamin A–replete and –depleted hosts, we identified the influence of RA signaling as acting on a single cell subtype.

Recently, two additional environmental factors besides RA have been identified that appear to influence the composition of cDC subsets within the spleen. These include induction of Notch signaling via the Notch2 receptor by the delta-like ligands and related members (Caton et al., 2007; Sekine et al., 2009; Lewis et al., 2011) and signaling through the G protein–coupled receptor EBI2 mediated by its ligand 7α,25-dihydroxycholesterol (Gatto et al., 2013). Interestingly, mice with the DC-specific deletion in the Notch2 receptor also have a defect in the SILP-associated $CD11b^+CD103^+$ population but no defects in peripheral LNs, phenocopying the cDC defects present in mice with impaired RA signaling. Previous studies in developmental biology have demonstrated that RA may augment Notch signaling both by increasing ligand availability (Wingert et al., 2007) as well as expression of the Notch receptors themselves (Mitsiadis et al., 1995). However, whether RA is acting in such a manner in adult mice to control the composition of cDCs or rather is acting in a Notch-independent manner remains to be determined (Stock and Bedoui, 2013).

We found that induction of mucosal injury through TBI caused an acute, dose-dependent VAD state in both mice and humans. In mice, this led to a reversible loss in the RA-dependent splenic $CD11b^+CD8\alpha^-Esam^{high}$ and SILP-associated $CD11b^+CD103^+$ cDC subset. These data therefore provide insight into a previously unrecognized mechanism by which TBI conditioning used in standard and experimental immunotherapies may induce unintended immunosuppression. Mechanistically, it is likely that radiation-induced mucosal injury blocks the normal enterohepatic circulation of the retinoids by preventing their reabsorption in the distal small bowel even as the retinoids are continuously being released at high concentrations through the bile (Jaensson-Gyllenbäck et al., 2011). Correlated with the selective loss of these DCs with enhanced class II Ag processing and presentation capacity after irradiation, we observed a loss in the efficacy of adoptively transferred, vaccine-stimulated $CD4^+$ but not $CD8^+$ T cells that was reversible with exogenous RA administration. Although we did not evaluate whether patients with irradiation-induced vitamin A depletion developed a circulating cDC defect in this manuscript, previous studies have demonstrated that RA and other RAR/RXR agonists can induce the terminal differentiation and Ag presentation capacity of human immature DCs (Geissmann et al., 2003; Mirza et al., 2006). Because RA is already an approved therapeutic reagent used to treat patients with a subset of acute myeloid leukemias (Tallman and Altman, 2009), these findings offer a potentially translatable clinical strategy to augment therapeutic vaccine- and T cell–based immunotherapies (Klebanoff et al., 2011a) and reverse irradiation-induced immune suppression. It will be of interest in future studies to determine whether other conditions that induce mucosal injury, such as parasitic worm infections (Grainger et al., 2013), HIV (Klatt et al., 2012), and graft versus host disease (Markey et al., 2012) may also induce a VAD state and an associated cDC-related immune deficiency.

In summary, we found that RA, an activated form of the essential nutrient vitamin A, plays an essential role in maintaining the homeostasis of pre-cDC–derived cDC subsets in both the spleen and gut. This occurs as RA influences the differentiation of the pre-cDCs between alternative fate commitments. In contrast, cDCs that are derived from monocytes and not pre-cDCs are not influenced by relative levels of RA signaling. These data provide an example of how a tumor-bearing host's nutritional status with respect to a single nutrient can critically impact cell-mediated immunity and extend RA's role in tuning immunity to include the regulation of DC homeostasis at both mucosal surfaces and in the spleen.

MATERIALS AND METHODS

Mouse strains, diets, and TBI. Adult (6–12 wk old) female C57BL/6 ($Ly5.2^+$), B6.FVB-Tg(Itgax-DTR/EGFP)57Lan/J (CD11c-DTR; Jung et al., 2002), B6.Cg-*Thy1*^{a}/Cy Tg(TcraTcrb)8Rest/J (Pmel-1) $CD8^+$ TCR transgenic (Overwijk et al., 2003), and B6.Cg-*Rag1*^{tm1Mom}*Tyrp1*$^{B-w}$Tg(Tcra, Tcrb)9Rest/J (Trp-1) $CD4^+$ TCR transgenic mice (Muranski et al., 2008; Muranski et al., 2011) were all purchased from The Jackson Laboratory. B6.SJL-*Ptprc*^{a}/BoyAiTac ($Ly5.1^+$) mice were purchased from Taconic. VAD and vitamin A–sufficient mice were generated as previously described (Hall et al., 2011a). In brief, beginning at day 14.5 of gestation, pregnant mice were initiated on either a VAD diet (TD.10991) or a similarly formulated Ctrl diet (20,000 IU vitamin A/kg; TD.10992), both purchased from Harlan Tekland Diets. Upon weaning, pups were continued on the diet until use (typically ≥12 wk). Per the manufacturer's recommendations, diets were stored at 4°C until use and replaced in the feed hopper every 3–4 d. Vitamin A deficiency was confirmed in a subset of mice by serum retinoid quantification, as described below. Where indicated, mice received the indicated doses of sublethal TBI without BM rescue. All mice were maintained under specific pathogen–free conditions, and animal experiments were conducted with the approval of the National Cancer Institute (NCI) and National Institute of Allergy and Infectious Disease Animal Use and Care Committees.

Quantitative RT-PCR and Western blot analysis of retinoid and rexinoid receptors from sorted cDC subsets. For quantitative RT-PCR analysis, cDC subsets were sorted directly into RNAprotect cell reagent, and RNA was extracted using the QiaShredders and RNeasy Mini kits (all from QIAGEN). cDNA was synthesized using the High Capacity RNA-to-cDNA kit (Applied Biosystems), and quantitative RT-PCR was performed on an ABI 7500 Fast instrument (Applied Biosystems) according to the manufacturer's protocol. Gene expression was quantified using commercially available probes targeting *Cd4*, *Cd8a*, *Rara*, *Rarb*, *Rarg*, *Rxra*, *Rxrb*, and *Rxrg* (Applied Biosystems). For Western blot analysis, splenic cDC subsets were sorted into FCS and subsequently lysed in RIPA buffer (Cell Signaling Technology) containing protease inhibitor. Protein was quantified using the Bio-Rad Laboratories protein assay. We separated 30 g of total protein on a 4–12% SDS-PAGE gel followed by standard immunoblotting with antibodies to RARα and RARγ (Cell Signaling Technology), Gapdh (EMD Millipore), and horseradish peroxidase–conjugated goat antibodies to mouse and rabbit IgG (Santa Cruz Biotechnology, Inc.). Blots were developed using chemiluminescence (Thermo Fisher Scientific) and acquired using the ChemiDoc system (Bio-Rad Laboratories).

BM chimeras and conditional depletion of CD11c-expressing cells. Generation of CD11c-DTR→Ly5.2 radiation chimeras were produced as described previously (Zammit et al., 2005). For conditional depletion of CD11c-expressing cells, mice were administered diphtheria toxin (4 ng/g/d; Sigma Aldrich) beginning 3 d before cell transfer and vaccination and then every 3 d thereafter, also as previously reported (Zammit et al., 2005). Diphtheria toxin was dissolved in DMSO (Sigma-Aldrich) and stored in single-use aliquots at −80°C.

Quantification of serum retinoids in humans and mice. Whole blood from human patients and mice was collected in darkened rooms under yellow light in serum separator tubes. Harvested specimens were placed on ice for 30 min to allow for clotting before serum separation by spinning at 10,000 *g* for 10 min. Serum was drawn off using a glass pipette, and aliquots were transferred into sterile Eppendorf tubes and snap frozen by immersion on dry ice before archiving in light-protected containers at −80°C. REs and *all-trans*-RA were extracted from serum as described previously (Kane et al., 2008a,b). REs were quantified by HPLC-UV detection (Kane et al., 2008a). RA was quantified by LC-tandem mass spectroscopy (Kane et al., 2008b). Retinoids were handled under yellow lights using only glass/stainless steel pipettes, syringes, and containers. Results were normalized per serum volume. Patient bio-specimen procurement was approved by the Institutional Review Board of the NCI, and participating patients provided written informed consent before participation in this study in accordance with the Declaration of Helsinki.

Spleen, LN, and SILP cell preparation. Spleens and iLNs were harvested from the indicated mice strains or treatment groups. Spleens were infused with 1 mg/ml type II collagenase (200 U/mg; Worthington Biochemical) and 15 µg/ml DNase (Roche) dissolved in complete media prewarmed to 37°C using 27 1/2–G needles (BD). After 10 min of incubation at 37°C, spleens and LNs were shredded and incubated for an additional 20 min at 37°C and then homogenized to a single-cell suspension by pipetting. After passage through a nylon mesh filter, cells were rested for 5 min and washed twice in a 1-mM EDTA-containing solution to disrupt DC–T cell complexes followed by removal of RBCs using ACK lysis buffer (Gibco). All subsequent steps were performed at 4°C in a 1-mM EDTA–containing solution of 0.5% (wt/wt) BSA (Sigma-Aldrich) dissolved in PBS. Isolation and analysis of DCs from the intestinal lamina propria was performed as described previously (Sun et al., 2007) with some modifications. In brief, after manual removal of Peyer's patches, small intestine segments were treated with medium containing 3% FCS and 20 mM Hepes (HyClone) for 20 min at 37°C with continuous stirring. Tissues were then further digested with 250 mg/ml Liberase TL (Roche) and 500 mg/ml DNase I (Sigma-Aldrich), also with continuous stirring at 37°C for 30 min. Digested tissue was forced through a Cellector tissue sieve (Bellco Glass, Inc.) and passed through 70- and 40-µm cell strainers. Cells were resuspended in 1.077 g/cm^3 iso-osmotic NycoPrep medium (Accurate Chemical & Scientific Corp.), and the low-density fraction was collected after centrifugation at 1,650 *g* for 15 min. Viable cells were counted either with a Countess automated cell counter using trypan blue exclusion or using CountBright beads (both from Invitrogen). In some experiments, CD11c$^+$ cells were pre-enriched before additional analysis by incubating with anti-CD11c microbeads (Miltenyi Biotec) for 10 min in the dark at 4°C followed by staining with fluorochrome-conjugated cell surface markers and then passage through a MACS selection column (Miltenyi Biotec).

RA agonists and antagonists. Where indicated, mice were administered either 250 µg per day of exogenous RA as previously described (Hall et al., 2011a) or DMSO vehicle Ctrl (both purchased from Sigma-Aldrich) by daily i.p. injection. In experiments in which mice received TBI, RA dosing was begun on day 3 after conditioning. The pan-RAR antagonist BMS493 (Tocris Bioscience) was administered at 220 µg per day as previously described (Kastner et al., 2001) by daily i.p. injection beginning 2 d before pre-cDC transfer and continuing until the day of progeny analysis or for 9–10 d for steady-state splenic immune subset evaluation. All reagents were dissolved in DMSO and stored in single-use aliquots at −80°C.

Pre-cDC isolation and adoptive transfer. BM-derived pre-cDCs were isolated as previously described (Liu et al., 2009) except for the following modifications: femurs and tibia of Ly5.2$^+$ mice were harvested and flushed, and RBCs were removed by ACK lysing buffer. After washing and filtering through nylon mesh, BM cells were pre-enriched for CD11c$^+$ cells as described above. After the positive fraction was eluted from columns (Miltenyi Biotec), propidium iodide was added, and viable pre-cDCs (B220$^-$CD3$^-$CD19$^-$NK1.1$^-$Ter119$^-$CD11c$^+$I-A/I-E$^-$Flt3$^+$Sirpα^{int}) were isolated to a purity of >95% by FACS sorting using a FACSAria (BD). In some experiments, pre-cDCs were derived from mice treated for 10 d with i.p. BMS493. Sorted pre-cDCs were washed twice with PBS before counting and transferring by i.v. injection 1.25–2 × 10^5 cells into nonirradiated Ly5.1 hosts maintained on the indicated diets or given exogenous RA or BM493. Pre-cDC progeny in the spleen were evaluated 6–7 d after transfer as done previously (Bogunovic et al., 2009; Ginhoux et al., 2009; Liu et al., 2009).

Flow cytometry staining and analysis. Spleen, LN, and BM-derived cells were isolated as described above and stained with fluorochrome-conjugated antibodies against combinations of the following surface Ags: B220 (RA3-6B2), CD3e (145-2C11), CD4 (GK1.5), CD8α (53-6.7), CD11b (M1/70), CD16/32 (2.4G2), CD19 (1D3), CD45.1 (NDS58), CD80 (16-10A1), CD86 (GL1), CD103 (M290), CD135/Flt3 (A2F10.1), CD172a/SIRPα (P84), H-2Db (KH95), Ki-67 (B56), NK1.1 (PK136), and Ter119 (TER-119; all from BD); CD11c (N418) and I-A/I-E (M5/114.15.2; both from BioLegend); and CD45 (30-F11), CD45.2 (104), CD205 (205yekta), CD317/mPDCA1 (eBio927), F4/80 (BM8), Ly6C (HK1.4), and Ly6G (RB6-8C5; all from eBioscience). For examination of cellular proliferation, cells were treated with the Foxp3 staining kit (eBioscience) per the manufacturer's instructions after surface Ag staining followed by staining for Ki67. Apoptosis was assessed using a fluorochrome-conjugated antibody to annexin V (556420; BD), also per the manufacturer's instructions. Cell viability was determined using propidium iodide exclusion in FACS-sorting experiments or fixable live/dead (Invitrogen) for diagnostic experiments. Flow cytometric data were acquired using either a FACSCanto II or LSRII cytometer (BD), and data were analyzed with FlowJo version 7.5 software (Tree Star).

Microarray analysis. DCs were pre-enriched from treated animals as described above and sorted into viable CD11c^{high}I-A/I-E$^+$CD11b$^+$CD8α$^-$ and CD11c^{high}I-A/I-E$^+$CD11b$^-$CD8α$^+$ subsets to a purity of >97% using a FACSAria cell sorter (BD). To maintain RNA integrity, cells were directly sorted into a 50/50 mixture of RNAprotect reagent (QIAGEN) and FCS. Sorted cells were centrifuged for 15 min at 2,000 rpm, and the cells were lysed using RLT buffer (QIAGEN). Total RNA was isolated from cells using

RNeasy Mini kits (QIAGEN) per the manufacturer's instructions. The quality of total RNA was evaluated using RNA 6000 Nano LabChip (2100 Bioanalyzer; Agilent Technologies). All samples had intact 18S and 28S ribosomal RNA bands with RIN numbers ranging from 7.3 to 9.3 and RNA 260/280 ratios between 1.9 and 2.1. Gene expression levels were determined using GeneChip Mouse Gene 1.0 ST arrays (Affymetrix) according to the manufacturer's protocols. Total tRNA (140 ng) was used as starting material for cDNA amplification and cRNA in vitro transcription (WT Expression kit; Ambion). cDNA fragments were labeled using the GeneChip WT Terminal Labeling kit (Affymetrix). Fragmented and labeled cDNA was hybridized on the arrays for 18 h according to the manufacturer's directions. Arrays were stained and washed in the Fluidics Station 400 (Affymetrix) and scanned (Affymetrix 7G). Arrays were preprocessed using Affymetrix's RMA-sketch procedures in Expression Console. One-way ANOVA was used to model each probe set and construct relevant pairwise comparisons. Differentially expressed probe sets were selected using a false discovery rate cutoff of 0.01 without specifying a fold change criterion. The data discussed in this manuscript have been deposited in NCBI's GEO database and are accessible through the GEO series accession no. GSE41021.

Assessment of ocular autoimmunity. Assessment of ocular autoimmunity was performed as described previously (Muranski et al., 2008; Palmer et al., 2008). In brief, eyes were enucleated at ≥3 wk after adoptive cell transfer, fixed in 10% formalin before embedding in methacrylate, and then sectioned along the papillary-optic nerve axis. The tissue was hematoxylin and eosin stained, and ocular autoimmunity was evaluated by an ophthalmological pathologist masked to the treatment group who assessed for iridiocyclitis, choroiditis, and vitritus using the following scoring schema: none = 0, mild = 1, moderate = 2, and severe = 3. The ocular autoimmunity score is presented as the sum of these three measurements. Bright-field images were acquired on an AF 6000 LX (Leica) using a 10× objective.

Assessment of antitumor immunity. Female C57BL/6 mice at 6–12 wk of age were implanted by s.c. injection with 4×10^5 B16 (H-2b) cells, a spontaneous $gp100^+/Trp\text{-}1^+$ mouse melanoma cell line obtained from the NCI tumor repository. 9 d later, all tumor-bearing mice received conditioning with 6 Gy TBI. Irradiated mice received RA or vehicle Ctrl by i.p. injection as described above. Treated mice received i.v. injection of 10^6 Pmel-1 $CD8^+$ or Trp-1 $CD4^+$ self/tumor-reactive T cells expanded in vitro for 6 d after enrichment by negative selection (Miltenyi Biotec) and activation under nonpolarizing conditions using 2 µg/ml each of plate-bound anti-CD3 and soluble anti-CD28 (both from BD) in complete media containing 4.4 ng/ml rhIL-2 (Novartis). Cells were administered in combination with 2×10^7 PFU of previously described rVVs encoding either hgp100 (rVVhgp100; Palmer et al., 2008) or Trp-1(rVVTrp-1; Muranski et al., 2008) along with 12 µg/dose of rhIL-2 administered twice daily by i.p. injection for a total of six doses (Klebanoff et al., 2011b). All tumor measurements were performed in a blinded fashion.

Statistics. The products of perpendicular tumor diameters were plotted as the mean ± SEM for each data point, and tumor treatment graphs were compared by using the Wilcoxon rank sum test. For all other experiments, data were compared using an unpaired Student's *t* test or χ^2 test. In all cases, p-values <0.05 were considered significant. All statistics were calculated using Prism 5 software (GraphPad Software).

Online supplemental material. Table S1, included as a separate Excel file, shows differentially expressed genes in $CD11b^+CD8\alpha^-$ and $CD11b^-CD8\alpha^+$ cDC subsets reconstituted after TBI in the presence of RA or vehicle Ctrl. Online supplemental material is available at http://www.jem.org/cgi/content/full/jem.20122508/DC1.

We thank all the members of the Restifo, Belkaid, and Germain laboratories for technical advice and thoughtful discussions, especially Z. Yu, S. Naik, W. Kastenmuller, and N. Subramanian. We thank C.C. Chan and members of the National Eye Institute, National Institutes of Health (NIH) tissue processing core laboratory for assistance with processing and analyzing ocular autoimmunity. We thank A. Mixon and S. Farid of the Flow Cytometry Unit for help with flow cytometry sorting. We thank S.A. Rosenberg, C. Laurencot, K. Morton, and M. Thompson for organization and assistance with procuring patient-related samples and S.A. Rosenberg for support of this project.

This work was supported by the Intramural Research Program of the National Cancer Institute, Center for Cancer Research of the US NIH, the NIH Office of Dietary Supplements (S.P. Spencer, J.R. Grainger, and J.A. Hall), NIH grant F30 DK094708-02 (to S.P. Spencer), and the Human Frontiers Science Program (C. Wilhelm).

The authors declare no competing financial interests.

Submitted: 9 November 2012
Accepted: 2 August 2013

REFERENCES

Aoyama, K., A. Saha, J. Tolar, M.J. Riddle, R.G. Veenstra, P.A. Taylor, R. Blomhoff, A. Panoskaltsis-Mortari, C.A. Klebanoff, G. Socie, et al. 2013. Inhibiting retinoic acid signaling ameliorates graft-versus-host disease by modifying T-cell differentiation and intestinal migration. *Blood*. http://dx.doi.org/10.1182/blood-2012-11-470252

Beijer, M.R., R. Molenaar, G. Goverse, R.E. Mebius, G. Kraal, and J.M. den Haan. 2013. A crucial role for retinoic acid in the development of Notch-dependent murine splenic CD8(-) CD4(-) and CD4(+) dendritic cells. *Eur. J. Immunol*. 43:1608–1616. http://dx.doi.org/10.1002/eji.201343325

Belz, G.T., and S.L. Nutt. 2012. Transcriptional programming of the dendritic cell network. *Nat. Rev. Immunol*. 12:101–113. http://dx.doi.org/10.1038/nri3149

Benson, M.J., K. Pino-Lagos, M. Rosemblatt, and R.J. Noelle. 2007. All-trans retinoic acid mediates enhanced T reg cell growth, differentiation, and gut homing in the face of high levels of co-stimulation. *J. Exp. Med*. 204:1765–1774. http://dx.doi.org/10.1084/jem.20070719

Blomhoff, R., and H.K. Blomhoff. 2006. Overview of retinoid metabolism and function. *J. Neurobiol*. 66:606–630. http://dx.doi.org/10.1002/neu.20242

Bogunovic, M., F. Ginhoux, J. Helft, L. Shang, D. Hashimoto, M. Greter, K. Liu, C. Jakubzick, M.A. Ingersoll, M. Leboeuf, et al. 2009. Origin of the lamina propria dendritic cell network. *Immunity*. 31:513–525. http://dx.doi.org/10.1016/j.immuni.2009.08.010

Caton, M.L., M.R. Smith-Raska, and B. Reizis. 2007. Notch-RBP-J signaling controls the homeostasis of CD8- dendritic cells in the spleen. *J. Exp. Med*. 204:1653–1664.

Coombes, J.L., K.R. Siddiqui, C.V. Arancibia-Cárcamo, J. Hall, C.M. Sun, Y. Belkaid, and F. Powrie. 2007. A functionally specialized population of mucosal $CD103^+$ DCs induces $Foxp3^+$ regulatory T cells via a TGF-β– and retinoic acid–dependent mechanism. *J. Exp. Med*. 204:1757–1764. http://dx.doi.org/10.1084/jem.20070590

Copelan, E.A. 2006. Hematopoietic stem-cell transplantation. *N. Engl. J. Med*. 354:1813–1826. http://dx.doi.org/10.1056/NEJMra052638

Dejardin, E., N.M. Droin, M. Delhase, E. Haas, Y. Cao, C. Makris, Z.W. Li, M. Karin, C.F. Ware, and D.R. Green. 2002. The lymphotoxin-beta receptor induces different patterns of gene expression via two NF-kappaB pathways. *Immunity*. 17:525–535. http://dx.doi.org/10.1016/S1074-7613(02)00423-5

den Haan, J.M., S.M. Lehar, and M.J. Bevan. 2000. $CD8^+$ but not $CD8^-$ dendritic cells cross-prime cytotoxic T cells in vivo. *J. Exp. Med*. 192:1685–1696. http://dx.doi.org/10.1084/jem.192.12.1685

DePaolo, R.W., V. Abadie, F. Tang, H. Fehlner-Peach, J.A. Hall, W. Wang, E.V. Marietta, D.D. Kasarda, T.A. Waldmann, J.A. Murray, et al. 2011. Co-adjuvant effects of retinoic acid and IL-15 induce inflammatory immunity to dietary antigens. *Nature*. 471:220–224. http://dx.doi.org/10.1038/nature09849

Dudley, M.E., J.C. Yang, R. Sherry, M.S. Hughes, R. Royal, U. Kammula, P.F. Robbins, J. Huang, D.E. Citrin, S.F. Leitman, et al. 2008. Adoptive cell therapy for patients with metastatic melanoma: evaluation of intensive myeloablative chemoradiation preparative regimens. *J. Clin. Oncol*. 26:5233–5239. http://dx.doi.org/10.1200/JCO.2008.16.5449

Dudziak, D., A.O. Kamphorst, G.F. Heidkamp, V.R. Buchholz, C. Trumpfheller, S. Yamazaki, C. Cheong, K. Liu, H.W. Lee, C.G. Park, et al. 2007. Differential antigen processing by dendritic cell subsets in vivo. *Science*. 315:107–111. http://dx.doi.org/10.1126/science.1136080

Gatto, D., K. Wood, I. Caminschi, D. Murphy-Durland, P. Schofield, D. Christ, G. Karupiah, and R. Brink. 2013. The chemotactic receptor EBI2 regulates the homeostasis, localization and immunological function of splenic dendritic cells. *Nat. Immunol.* 14:446–453. http://dx.doi.org/10.1038/ni.2555

Geissmann, F., P. Revy, N. Brousse, Y. Lepelletier, C. Folli, A. Durandy, P. Chambon, and M. Dy. 2003. Retinoids regulate survival and antigen presentation by immature dendritic cells. *J. Exp. Med.* 198:623–634. http://dx.doi.org/10.1084/jem.20030390

Germain, P., C. Gaudon, V. Pogenberg, S. Sanglier, A. Van Dorsselaer, C.A. Royer, M.A. Lazar, W. Bourguet, and H. Gronemeyer. 2009. Differential action on coregulator interaction defines inverse retinoid agonists and neutral antagonists. *Chem. Biol.* 16:479–489. http://dx.doi.org/10.1016/j.chembiol.2009.03.008

Ginhoux, F., K. Liu, J. Helft, M. Bogunovic, M. Greter, D. Hashimoto, J. Price, N. Yin, J. Bromberg, S.A. Lira, et al. 2009. The origin and development of nonlymphoid tissue CD103$^+$ DCs. *J. Exp. Med.* 206:3115–3130. http://dx.doi.org/10.1084/jem.20091756

Grainger, J.R., E.A. Wohlfert, I.J. Fuss, N. Bouladoux, M.H. Askenase, F. Legrand, L.Y. Koo, J.M. Brenchley, I.D. Fraser, and Y. Belkaid. 2013. Inflammatory monocytes regulate pathologic responses to commensals during acute gastrointestinal infection. *Nat. Med.* 19:713–721. http://dx.doi.org/10.1038/nm.3189

Hall, J.A., J.L. Cannons, J.R. Grainger, L.M. Dos Santos, T.W. Hand, S. Naik, E.A. Wohlfert, D.B. Chou, G. Oldenhove, M. Robinson, et al. 2011a. Essential role for retinoic acid in the promotion of CD4(+) T cell effector responses via retinoic acid receptor alpha. *Immunity*. 34:435–447. http://dx.doi.org/10.1016/j.immuni.2011.03.003

Hall, J.A., J.R. Grainger, S.P. Spencer, and Y. Belkaid. 2011b. The role of retinoic acid in tolerance and immunity. *Immunity*. 35:13–22. http://dx.doi.org/10.1016/j.immuni.2011.07.002

Iwata, M., A. Hirakiyama, Y. Eshima, H. Kagechika, C. Kato, and S.Y. Song. 2004. Retinoic acid imprints gut-homing specificity on T cells. *Immunity*. 21:527–538. http://dx.doi.org/10.1016/j.immuni.2004.08.011

Jaensson-Gyllenbäck, E., K. Kotarsky, F. Zapata, E.K. Persson, T.E. Gundersen, R. Blomhoff, and W.W. Agace. 2011. Bile retinoids imprint intestinal CD103+ dendritic cells with the ability to generate gut-tropic T cells. *Mucosal Immunol.* 4:438–447. http://dx.doi.org/10.1038/mi.2010.91

Jung, S., D. Unutmaz, P. Wong, G. Sano, K. De los Santos, T. Sparwasser, S. Wu, S. Vuthoori, K. Ko, F. Zavala, et al. 2002. In vivo depletion of CD11c+ dendritic cells abrogates priming of CD8+ T cells by exogenous cell-associated antigens. *Immunity*. 17:211–220. http://dx.doi.org/10.1016/S1074-7613(02)00365-5

Kabashima, K., T.A. Banks, K.M. Ansel, T.T. Lu, C.F. Ware, and J.G. Cyster. 2005. Intrinsic lymphotoxin-beta receptor requirement for homeostasis of lymphoid tissue dendritic cells. *Immunity*. 22:439–450. http://dx.doi.org/10.1016/j.immuni.2005.02.007

Kamphorst, A.O., P. Guermonprez, D. Dudziak, and M.C. Nussenzweig. 2010. Route of antigen uptake differentially impacts presentation by dendritic cells and activated monocytes. *J. Immunol.* 185:3426–3435. http://dx.doi.org/10.4049/jimmunol.1001205

Kane, M.A., A.E. Folias, and J.L. Napoli. 2008a. HPLC/UV quantitation of retinal, retinol, and retinyl esters in serum and tissues. *Anal. Biochem.* 378:71–79. http://dx.doi.org/10.1016/j.ab.2008.03.038

Kane, M.A., A.E. Folias, C. Wang, and J.L. Napoli. 2008b. Quantitative profiling of endogenous retinoic acid in vivo and in vitro by tandem mass spectrometry. *Anal. Chem.* 80:1702–1708. http://dx.doi.org/10.1021/ac702030f

Kastner, P., H.J. Lawrence, C. Waltzinger, N.B. Ghyselinck, P. Chambon, and S. Chan. 2001. Positive and negative regulation of granulopoiesis by endogenous RARalpha. *Blood*. 97:1314–1320. http://dx.doi.org/10.1182/blood.V97.5.1314

Klatt, N.R., J.D. Estes, X. Sun, A.M. Ortiz, J.S. Barber, L.D. Harris, B. Cervasi, L.K. Yokomizo, L. Pan, C.L. Vinton, et al. 2012. Loss of mucosal CD103+ DCs and IL-17+ and IL-22+ lymphocytes is associated with mucosal damage in SIV infection. *Mucosal Immunol.* 5:646–657. http://dx.doi.org/10.1038/mi.2012.38

Klebanoff, C.A., H.T. Khong, P.A. Antony, D.C. Palmer, and N.P. Restifo. 2005. Sinks, suppressors and antigen presenters: how lymphodepletion enhances T cell-mediated tumor immunotherapy. *Trends Immunol.* 26:111–117. http://dx.doi.org/10.1016/j.it.2004.12.003

Klebanoff, C.A., N. Acquavella, Z. Yu, and N.P. Restifo. 2011a. Therapeutic cancer vaccines: are we there yet? *Immunol. Rev.* 239:27–44. http://dx.doi.org/10.1111/j.1600-065X.2010.00979.x

Klebanoff, C.A., L. Gattinoni, D.C. Palmer, P. Muranski, Y. Ji, C.S. Hinrichs, Z.A. Borman, S.P. Kerkar, C.D. Scott, S.E. Finkelstein, et al. 2011b. Determinants of successful CD8+ T-cell adoptive immunotherapy for large established tumors in mice. *Clin. Cancer Res.* 17:5343–5352. http://dx.doi.org/10.1158/1078-0432.CCR-11-0503

Kuwata, T., I.M. Wang, T. Tamura, R.M. Ponnamperuma, R. Levine, K.L. Holmes, H.C. Morse, L.M. De Luca, and K. Ozato. 2000. Vitamin A deficiency in mice causes a systemic expansion of myeloid cells. *Blood*. 95:3349–3356.

Lewis, K.L., M.L. Caton, M. Bogunovic, M. Greter, L.T. Grajkowska, D. Ng, A. Klinakis, I.F. Charo, S. Jung, J.L. Gommerman, et al. 2011. Notch2 receptor signaling controls functional differentiation of dendritic cells in the spleen and intestine. *Immunity*. 35:780–791. http://dx.doi.org/10.1016/j.immuni.2011.08.013

Liu, K., G.D. Victora, T.A. Schwickert, P. Guermonprez, M.M. Meredith, K. Yao, F.F. Chu, G.J. Randolph, A.Y. Rudensky, and M. Nussenzweig. 2009. In vivo analysis of dendritic cell development and homeostasis. *Science*. 324:392–397. http://dx.doi.org/10.1126/science.1170540

Markey, K.A., M. Koyama, R.D. Kuns, K.E. Lineburg, Y.A. Wilson, S.D. Olver, N.C. Raffelt, A.L. Don, A. Varelias, R.J. Robb, et al. 2012. Immune insufficiency during GVHD is due to defective antigen presentation within dendritic cell subsets. *Blood*. 119:5918–5930. http://dx.doi.org/10.1182/blood-2011-12-398164

Merad, M., P. Sathe, J. Helft, J. Miller, and A. Mortha. 2013. The dendritic cell lineage: ontogeny and function of dendritic cells and their subsets in the steady state and the inflamed setting. *Annu. Rev. Immunol.* 31:563–604. http://dx.doi.org/10.1146/annurev-immunol-020711-074950

Mielke, L.A., S.A. Jones, M. Raverdeau, R. Higgs, A. Stefanska, J.R. Groom, A. Misiak, L.S. Dungan, C.E. Sutton, G. Streubel, et al. 2013. Retinoic acid expression associates with enhanced IL-22 production by γδ T cells and innate lymphoid cells and attenuation of intestinal inflammation. *J. Exp. Med.* 210:1117–1124. http://dx.doi.org/10.1084/jem.20121588

Miller, J.C., B.D. Brown, T. Shay, E.L. Gautier, V. Jojic, A. Cohain, G. Pandey, M. Leboeuf, K.G. Elpek, J. Helft, et al; Immunological Genome Consortium. 2012. Deciphering the transcriptional network of the dendritic cell lineage. *Nat. Immunol.* 13:888–899. http://dx.doi.org/10.1038/ni.2370

Mirza, N., M. Fishman, I. Fricke, M. Dunn, A.M. Neuger, T.J. Frost, R.M. Lush, S. Antonia, and D.I. Gabrilovich. 2006. All-trans-retinoic acid improves differentiation of myeloid cells and immune response in cancer patients. *Cancer Res.* 66:9299–9307. http://dx.doi.org/10.1158/0008-5472.CAN-06-1690

Mitsiadis, T.A., M. Lardelli, U. Lendahl, and I. Thesleff. 1995. Expression of Notch 1, 2 and 3 is regulated by epithelial-mesenchymal interactions and retinoic acid in the developing mouse tooth and associated with determination of ameloblast cell fate. *J. Cell Biol.* 130:407–418. http://dx.doi.org/10.1083/jcb.130.2.407

Mora, J.R., M. Iwata, B. Eksteen, S.Y. Song, T. Junt, B. Senman, K.L. Otipoby, A. Yokota, H. Takeuchi, P. Ricciardi-Castagnoli, et al. 2006. Generation of gut-homing IgA-secreting B cells by intestinal dendritic cells. *Science*. 314:1157–1160. http://dx.doi.org/10.1126/science.1132742

Mora, J.R., M. Iwata, and U.H. von Andrian. 2008. Vitamin effects on the immune system: vitamins A and D take centre stage. *Nat. Rev. Immunol.* 8:685–698. http://dx.doi.org/10.1038/nri2378

Mucida, D., Y. Park, G. Kim, O. Turovskaya, I. Scott, M. Kronenberg, and H. Cheroutre. 2007. Reciprocal TH17 and regulatory T cell differentiation mediated by retinoic acid. *Science*. 317:256–260. http://dx.doi.org/10.1126/science.1145697

Muranski, P., A. Boni, P.A. Antony, L. Cassard, K.R. Irvine, A. Kaiser, C.M. Paulos, D.C. Palmer, C.E. Touloukian, K. Ptak, et al. 2008. Tumor-specific

Th17-polarized cells eradicate large established melanoma. *Blood*. 112: 362–373. http://dx.doi.org/10.1182/blood-2007-11-120998

Muranski, P., Z.A. Borman, S.P. Kerkar, C.A. Klebanoff, Y. Ji, L. Sanchez-Perez, M. Sukumar, R.N. Reger, Z.Yu, S.J. Kern, et al. 2011. Th17 cells are long lived and retain a stem cell-like molecular signature. *Immunity*. 35:972–985. http://dx.doi.org/10.1016/j.immuni.2011.09.019

Naik, S.H., D. Metcalf, A. van Nieuwenhuijze, I. Wicks, L. Wu, M. O'Keeffe, and K. Shortman. 2006. Intrasplenic steady-state dendritic cell precursors that are distinct from monocytes. *Nat. Immunol.* 7:663–671. http://dx.doi.org/10.1038/ni1340

Napoli, J.L. 2012. Physiological insights into all-trans-retinoic acid biosynthesis. *Biochim. Biophys. Acta*. 1821:152–167. http://dx.doi.org/10.1016/j.bbalip.2011.05.004

Niederreither, K., and P. Dollé. 2008. Retinoic acid in development: towards an integrated view. *Nat. Rev. Genet*. 9:541–553. http://dx.doi.org/10.1038/nrg2340

Overwijk, W.W., M.R. Theoret, S.E. Finkelstein, D.R. Surman, L.A. de Jong, F.A. Vyth-Dreese, T.A. Dellemijn, P.A. Antony, P.J. Spiess, D.C. Palmer, et al. 2003. Tumor regression and autoimmunity after reversal of a functionally tolerant state of self-reactive CD8+ T cells. *J. Exp. Med*. 198:569–580. http://dx.doi.org/10.1084/jem.20030590

Palmer, D.C., C.C. Chan, L. Gattinoni, C. Wrzesinski, C.M. Paulos, C.S. Hinrichs, D.J. Powell Jr., C.A. Klebanoff, S.E. Finkelstein, R.N. Fariss, et al. 2008. Effective tumor treatment targeting a melanoma/melanocyte-associated antigen triggers severe ocular autoimmunity. *Proc. Natl. Acad. Sci. USA*. 105:8061–8066. http://dx.doi.org/10.1073/pnas.0710929105

Paulos, C.M., C. Wrzesinski, A. Kaiser, C.S. Hinrichs, M. Chieppa, L. Cassard, D.C. Palmer, A. Boni, P. Muranski, Z.Yu, et al. 2007. Microbial translocation augments the function of adoptively transferred self/tumor-specific CD8+ T cells via TLR4 signaling. *J. Clin. Invest.* 117:2197–2204. http://dx.doi.org/10.1172/JCI32205

Pino-Lagos, K., Y. Guo, C. Brown, M.P. Alexander, R. Elgueta, K.A. Bennett, V. De Vries, E. Nowak, R. Blomhoff, S. Sockanathan, et al. 2011. A retinoic acid–dependent checkpoint in the development of $CD4^+$ T cell–mediated immunity. *J. Exp. Med*. 208:1767–1775. http://dx.doi.org/10.1084/jem.20102358

Pooley, J.L., W.R. Heath, and K. Shortman. 2001. Cutting edge: intravenous soluble antigen is presented to CD4 T cells by CD8- dendritic cells, but cross-presented to CD8 T cells by CD8+ dendritic cells. *J. Immunol*. 166:5327–5330.

Satpathy, A.T., W. Kc, J.C. Albring, B.T. Edelson, N.M. Kretzer, D. Bhattacharya, T.L. Murphy, and K.M. Murphy. 2012. *Zbtb46* expression distinguishes classical dendritic cells and their committed progenitors from other immune lineages. *J. Exp. Med*. 209:1135–1152. http://dx.doi.org/10.1084/jem.20120030

Sekine, C., Y. Moriyama, A. Koyanagi, N. Koyama, H. Ogata, K. Okumura, and H. Yagita. 2009. Differential regulation of splenic CD8- dendritic cells and marginal zone B cells by Notch ligands. *Int. Immunol*. 21:295–301. http://dx.doi.org/10.1093/intimm/dxn148

Semba, R.D. 1999. Vitamin A as "anti-infective" therapy, 1920-1940. *J. Nutr*. 129:783–791.

Stock, A.T., and S. Bedoui. 2013. Vitamin A notches up CD11b(hi) DC development. *Eur. J. Immunol*. 43:1441–1444. http://dx.doi.org/10.1002/eji.201343631

Sun, C.M., J.A. Hall, R.B. Blank, N. Bouladoux, M. Oukka, J.R. Mora, and Y. Belkaid. 2007. Small intestine lamina propria dendritic cells promote de novo generation of Foxp3 T reg cells via retinoic acid. *J. Exp. Med*. 204:1775–1785. http://dx.doi.org/10.1084/jem.20070602

Tallman, M.S., and J.K. Altman. 2009. How I treat acute promyelocytic leukemia. *Blood*. 114:5126–5135. http://dx.doi.org/10.1182/blood-2009-07-216457

Trier, J.S., and T.H. Browning. 1966. Morphologic response of the mucosa of human small intestine to x-ray exposure. *J. Clin. Invest*. 45:194–204. http://dx.doi.org/10.1172/JCI105332

Varol, C., L. Landsman, D.K. Fogg, L. Greenshtein, B. Gildor, R. Margalit, V. Kalchenko, F. Geissmann, and S. Jung. 2007. Monocytes give rise to mucosal, but not splenic, conventional dendritic cells. *J. Exp. Med*. 204:171–180. http://dx.doi.org/10.1084/jem.20061011

Varol, C., A. Vallon-Eberhard, E. Elinav, T. Aychek, Y. Shapira, H. Luche, H.J. Fehling, W.D. Hardt, G. Shakhar, and S. Jung. 2009. Intestinal lamina propria dendritic cell subsets have different origin and functions. *Immunity*. 31:502–512. http://dx.doi.org/10.1016/j.immuni.2009.06.025

Wingert, R.A., R. Selleck, J. Yu, H.D. Song, Z. Chen, A. Song, Y. Zhou, B. Thisse, C. Thisse, A.P. McMahon, and A.J. Davidson. 2007. The cdx genes and retinoic acid control the positioning and segmentation of the zebrafish pronephros. *PLoS Genet*. 3:e189. http://dx.doi.org/10.1371/journal.pgen.0030189

Wu, L., A. D'Amico, K.D. Winkel, M. Suter, D. Lo, and K. Shortman. 1998. RelB is essential for the development of myeloid-related CD8alpha- dendritic cells but not of lymphoid-related CD8alpha+ dendritic cells. *Immunity*. 9:839–847. http://dx.doi.org/10.1016/S1074-7613(00)80649-4

Zammit, D.J., L.S. Cauley, Q.M. Pham, and L. Lefrançois. 2005. Dendritic cells maximize the memory CD8 T cell response to infection. *Immunity*. 22:561–570. http://dx.doi.org/10.1016/j.immuni.2005.03.005

Zhang, Y., J.P. Louboutin, J. Zhu, A.J. Rivera, and S.G. Emerson. 2002. Preterminal host dendritic cells in irradiated mice prime CD8+ T cell-mediated acute graft-versus-host disease. *J. Clin. Invest*. 109:1335–1344.